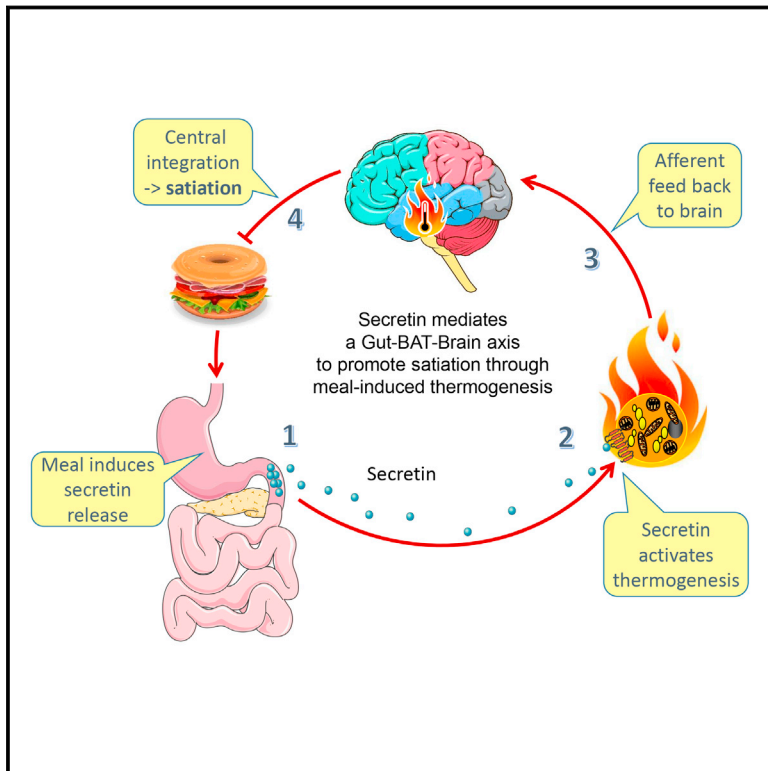


Secretin-Activated Brown Fat Mediates Prandial Thermogenesis to Induce Satiation

Graphical Abstract



Authors

Yongguo Li, Katharina Schnabl, Sarah-Madeleine Gabler, ..., Vasilis Ntziachristos, Pirjo Nuutila, Martin Klingenspor

Correspondence

mk@tum.de

In Brief

Secretin, a gut hormone secreted while eating a meal, stimulates brown fat thermogenesis and induction of satiation in mice and humans.

Highlights

- Secretin receptor (SCTR) is highly expressed in BAT
- Secretin activates BAT thermogenesis through SCTR-PKA-ATGL/HSL pathway
- Secretin-activated BAT mediates prandial thermogenesis and induces satiation
- Secretin activates human BAT



Secretin-Activated Brown Fat Mediates Prandial Thermogenesis to Induce Satiation

Yongguo Li,^{1,2,9} Katharina Schnabl,^{1,2,3,9} Sarah-Madeleine Gabler,^{1,2,3} Monja Willershäuser,^{1,2} Josefine Reber,^{4,5} Angelos Karlas,^{4,5} Sanna Laurila,⁶ Minna Lahesmaa,⁶ Mueez u Din,⁶ Andrea Bast-Habersbrunner,^{1,2} Kirsi A. Virtanen,⁶ Tobias Fromme,^{1,2,3} Florian Bolze,^{1,2} Libbey S. O'Farrell,⁷ Jorge Alsina-Fernandez,⁷ Tamer Coskun,⁷ Vasilis Ntziachristos,^{4,5} Pirjo Nuutila,^{6,8} and Martin Klingenspor^{1,2,3,10,*}

¹Chair for Molecular Nutritional Medicine, TUM School of Life Sciences, Technical University of Munich, Freising, Germany

²EKFZ – Else Kröner-Fresenius Center for Nutritional Medicine, Technical University of Munich, Freising, Germany

³ZIEL – Institute for Food & Health, Technical University of Munich, Freising, Germany

⁴Institute for Biological and Medical Imaging (IBMI), Helmholtz Zentrum München, Neuherberg

⁵Chair for Biological Imaging, Technical University of Munich, Munich, Germany

⁶Turku PET Centre, University of Turku, Turku, Finland

⁷Lilly Research Laboratories, Lilly Corporate Center, Indianapolis, IN, USA

⁸Department of Endocrinology, Turku University Hospital, Turku, Finland

⁹These authors contributed equally

¹⁰Lead Contact

*Correspondence: mk@tum.de

<https://doi.org/10.1016/j.cell.2018.10.016>

SUMMARY

The molecular mediator and functional significance of meal-associated brown fat (BAT) thermogenesis remains elusive. Here, we identified the gut hormone secretin as a non-sympathetic BAT activator mediating prandial thermogenesis, which consequently induces satiation, thereby establishing a gut-secretin-BAT-brain axis in mammals with a physiological role of prandial thermogenesis in the control of satiation. Mechanistically, meal-associated rise in circulating secretin activates BAT thermogenesis by stimulating lipolysis upon binding to secretin receptors in brown adipocytes, which is sensed in the brain and promotes satiation. Chronic infusion of a modified human secretin transiently elevates energy expenditure in diet-induced obese mice. Clinical trials with human subjects showed that thermogenesis after a single-meal ingestion correlated with postprandial secretin levels and that secretin infusions increased glucose uptake in BAT. Collectively, our findings highlight the largely unappreciated function of BAT in the control of satiation and qualify BAT as an even more attractive target for treating obesity.

INTRODUCTION

In mammals, white adipose tissue (WAT) stores fat as the major energy backup for times of limited food supply, whereas brown adipose tissue (BAT) generates heat in response to cold exposure (Rosen and Spiegelman, 2006). Thermogenesis in BAT, known as non-shivering thermogenesis, dissipates chemical

energy of nutrients by uncoupling oxygen consumption from ATP synthesis in mitochondria (Klingenspor, 2003). This mechanism depends on the uncoupling protein 1 (UCP1). Cold exposure activates BAT and leads to the recruitment of thermogenic capacity (Cannon and Nedergaard, 2004).

The discovery of cold-induced BAT activity in adult humans, attenuated with age, insulin resistance, diabetes, and obesity, has attained large interest (Sidossis and Kajimura, 2015). Cold acclimation recruits BAT activity (Blondin et al., 2014; van der Lans et al., 2013) and improves insulin sensitivity (Chondronikola et al., 2014; Hanssen et al., 2015), body fat mass (Yoneshiro et al., 2013), and hypercholesterolemia (Berbée et al., 2015). It is unclear, however, whether the total catabolic capacity of BAT is sufficient to account for these beneficial metabolic effects (Blondin et al., 2017; Hanssen et al., 2015).

BAT also contributes to meal-associated thermogenesis (Glick et al., 1981; Saito, 2013; U Din et al., 2018; Vosselman et al., 2013) and to long-term diet-induced thermogenesis (Rothwell and Stock, 1979). Meal-associated thermogenesis, when regarding a single meal, maybe divided into three phases: a pre-prandial, a prandial, and a postprandial phase. The contribution of BAT thermogenesis to these three phases is unclear. Furthermore, the molecular mediators and functional significance of meal-associated BAT thermogenesis are poorly understood. It is generally believed that an increased periprandial tone of the sympathetic nervous system (SNS) stimulates norepinephrine release from sympathetic nerves in BAT and activates canonical cAMP-PKA (cyclic AMP-protein kinase A) signaling via β 3-adrenergic receptors (β 3-ARs). This pathway activates lipolysis, UCP1, and non-shivering thermogenesis (Cannon and Nedergaard, 2004). Notably, meal-associated thermogenesis in BAT may promote central perception of satiation (Blessing et al., 2013; Brobeck, 1948; Glick, 1982; Himms-Hagen, 1995). In fasted mice, acute pharmacological BAT activation with a β 3-AR agonist reduces cumulative food intake during refeeding (Grujic et al., 1997; Susulic et al., 1995).



All macronutrients elicit meal-associated thermogenesis, but only carbohydrate activates the SNS (Glick, 1982; Himms-Hagen, 1995; Welle et al., 1981). Notably, blockade of β -ARs with propranolol does not attenuate the early meal-associated rise in whole-body heat production caused by a carbohydrate meal or a mixed carbohydrate-rich meal (Astrup et al., 1989; Thörne and Wahren, 1989; Zwillich et al., 1981). We therefore hypothesized that not only catecholamines but also one of the gut hormones secreted into circulation during a meal may directly activate BAT. Secretion of gut hormones during a meal encodes information on the nutritional status and coordinates gastrointestinal motility and secretion for digestion and resorption, and it also controls the central perception of satiation and satiety in the brain via enteric neuronal afferent and endocrine feedback pathways (Chaudhri et al., 2006). In addition, periprandial secretion of gut hormones, like cholecystokinin (CCK) and glucagon-like peptide 1 (GLP-1), stimulates the central efferent tone of sympathetic innervation in BAT and thereby activates meal-associated non-shivering thermogenesis (Beiroa et al., 2014; Blouet and Schwartz, 2012). Furthermore, gut hormones directly modulate triglyceride metabolism in adipocytes. For example, the gut hormone peptide YY (PYY) inhibits lipolysis via Y2R coupled to G_i signaling (Valet et al., 1990), and secretin stimulates lipolysis through the secretin receptor (*Sctr*) coupled to G_s (Braun et al., 2018). As lipolysis is an essential prerequisite of BAT thermogenesis, we therefore set out to identify gut hormones that directly activate meal-associated thermogenesis in BAT and control satiation.

RESULTS

Abundant Expression of the Secretin Receptor in Brown Adipocytes

In a first step, we profiled gene expression of gut hormone receptors by inquiring transcriptome data obtained from interscapular BAT (iBAT) tissue of mice (GSE119452). Among the detectable transcripts of gut hormone receptor genes in iBAT, the secretin receptor (*Sctr*) stood out with the highest transcript abundance compared to other gut hormone receptors (Figure 1A). Our qPCR analyses revealed that *Sctr* is more abundantly expressed in iBAT compared to inguinal (iWAT) and epididymal (eWAT) white adipose tissue (Figure 1B). Preferential *Sctr* expression in brown adipocytes was also observed in primary cultures derived from these fat depots (Figure 1C). The Online Biology Gene Portal System (BioGPS) also detects *Sctr* as highly expressed in BAT (Figure S1).

Sctr gene expression predominated in mature brown adipocytes compared to undifferentiated stromal vascular cells (SVF) (Figure 1D), and differentiation of brown adipocytes was associated with an increase in *Sctr* at the transcript (Figure 1E) and at the protein level (Figure 1F). SCTR is a G_s protein-coupled GPCR (G-protein-coupled receptor) receptor of the class II receptor family (Afroze et al., 2013). Upon secretin binding, SCTR activates lipolysis by cAMP-PKA signaling in murine white adipocytes (Braun et al., 2018). In brown adipocytes, free fatty acids released by lipolysis serve as activators of UCP1 and substrates for thermogenesis. Moreover, secretin was reported to stimulate oxygen consumption in rat brown adipocytes (Dicker

et al., 1998). Therefore, we postulated that SCTR in brown adipocytes may activate UCP1-mediated thermogenesis upon binding of secretin.

Secretin Activates Thermogenesis

To test whether secretin can activate thermogenesis, we measured UCP1-mediated thermogenesis in cultured adherent primary brown adipocytes (Li et al., 2014). We observed that secretin at a 50-fold lower concentration is as potent as isoproterenol (ISO), a β -AR agonist, in stimulating thermogenesis (Figures 2A and 2B). The minimal concentration to stimulate thermogenesis in brown adipocytes was 0.1 nM for secretin (Figure S2A) but at least 10 nM for ISO (Figure S2B). In dose-response experiments, EC_{50} values for secretin and ISO were 0.13 nM and 23.4 nM, respectively (Figure S2C). The thermogenic effect of secretin was independent of ARs, since pretreatment of brown adipocytes with propranolol, a nonselective β -AR antagonist, did not attenuate secretin-stimulated respiration while blocking the effect of ISO in a dose-dependent manner (Figure 2C). The thermogenic effect of secretin, however, depends on SCTR, as small interfering RNA (siRNA)-mediated downregulation of receptor expression (Figure S2G) blunted the effects of secretin on oxygen consumption (Figure 2D). Secretin stimulation resulted in a dose-dependent increase of relative cytosolic cAMP levels in brown adipocytes (Figure S2D). Pretreatment of cells with H89, a selective inhibitor of PKA (Figure 2E), or inhibitors targeting the two key lipases involved in lipolysis (adipose triglyceride lipase, ATGL; hormone-sensitive lipase, HSL), completely blocked the thermogenic effect of secretin (Figure 2F). This demonstrates that secretin-induced thermogenesis depends on the activation of lipolysis through the canonical cAMP-PKA pathway. Secretin also increased thermogenic gene expression in brown and white adipocytes (Figures S2E and S2F). Together, these data reveal a novel physiological role of secretin, serving as a non-adrenergic activator of thermogenesis.

We next tested whether secretin could induce thermogenesis *in vivo* using indirect calorimetry. A single intraperitoneal (i.p.) injection of secretin increased heat production in wild-type (WT) mice but not in UCP1 knockout (KO) mice (Figures 2G–2I). The thermogenic secretin effect in WT mice was maintained at thermoneutrality (TN, 30°C), and the magnitude is comparable to noradrenaline (Figures 2J and 2K), which was confirmed by a corresponding rise in iBAT temperature (Figure 2L). To further visualize BAT activation, we applied indirect calorimetry with multispectral optoacoustic tomography (MSOT) in nude mice, which detects the spectra of oxygenated and deoxygenated hemoglobin in high resolution deep in tissues and blood vessels (Reber et al., 2018). By monitoring the Sulzer's vein, the only venous drainage of iBAT, we found that total blood volume (TBV) was increased whereas relative oxygen saturation (SO_2) was dramatically decreased after secretin stimulation (Figures 2M–2P). Thus, secretin activates iBAT thermogenesis *in vivo*.

Secretin-Activated BAT Induces Satiation

Plasma secretin levels were decreased by fasting (18 hr) and increased significantly within 1 hr after refeeding (Figure 3A), which is congruent with changes of iBAT temperature (Figure 3B).

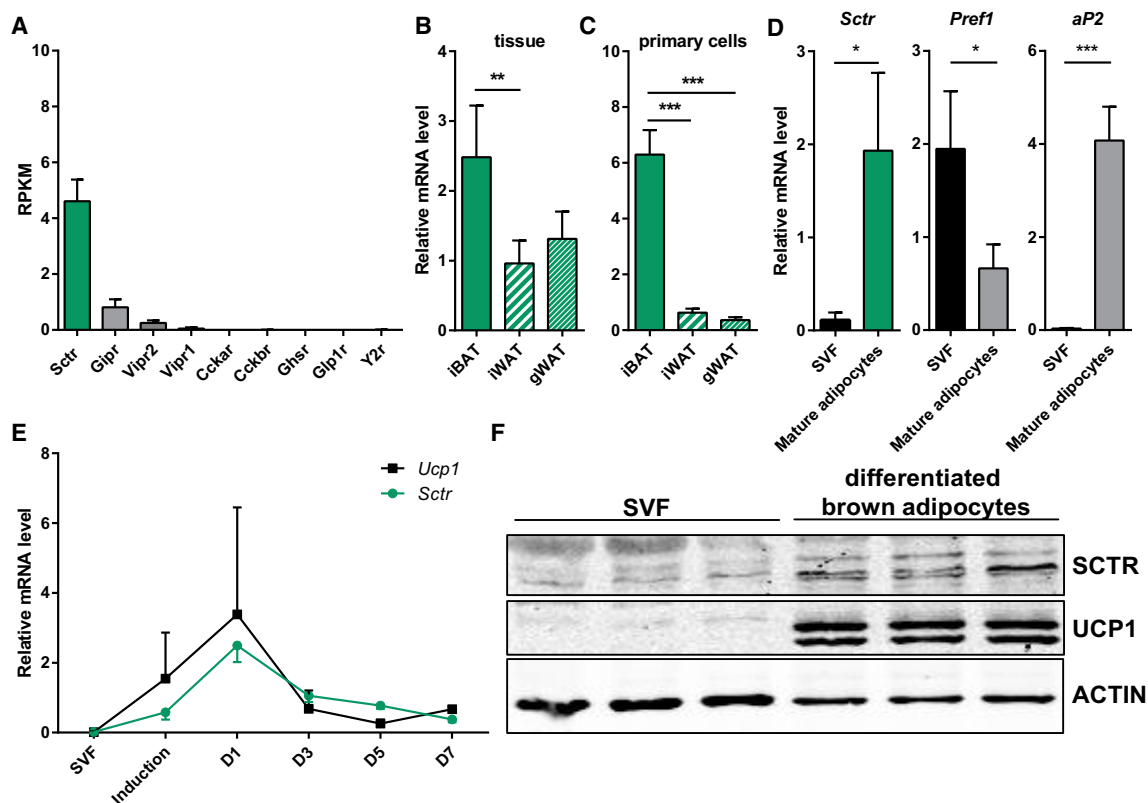


Figure 1. Secretin Receptor Is Highly Expressed in Murine BAT

(A) Profiling of gut hormone receptors expressed in murine brown adipose tissue (BAT) using RNA sequencing (RNA-seq) data. Data are shown as RPKM (reads per kilobase per million mapped reads). Secretin receptor (*Sctr*) stood out with the highest transcript abundance compared to other gut hormone receptors such as gastric inhibitory polypeptide receptor (*Gipr*), vasoactive intestinal peptide receptor1/2 (*Vipr1/2*), cholecystokinin A/B receptor (*Cckar/br*), ghrelin receptor (*Ghsr*), glucagon-like peptide 1 receptor (*Glp1r*), and the PYY₃₋₃₆ receptor (*Npy2r*) (n = 4).

(B and C) Relative expression levels of *Sctr* in BAT and inguinal (iWAT) and epididymal (eWAT) white adipose tissues as well as primary cultures (C) derived from these fat depots assessed by qPCR (n = 5).

(D) Relative expression abundance of *Sctr*, *Pref1* (preadipocyte factor 1), and *aP2* (adipocyte protein 2) in stromal vascular fraction (SVF) and mature adipocytes (n = 3).

(E) Time course expression of uncoupling protein 1 (*Ucp1*) and *Sctr* mRNA during brown adipocyte differentiation (n = 3).

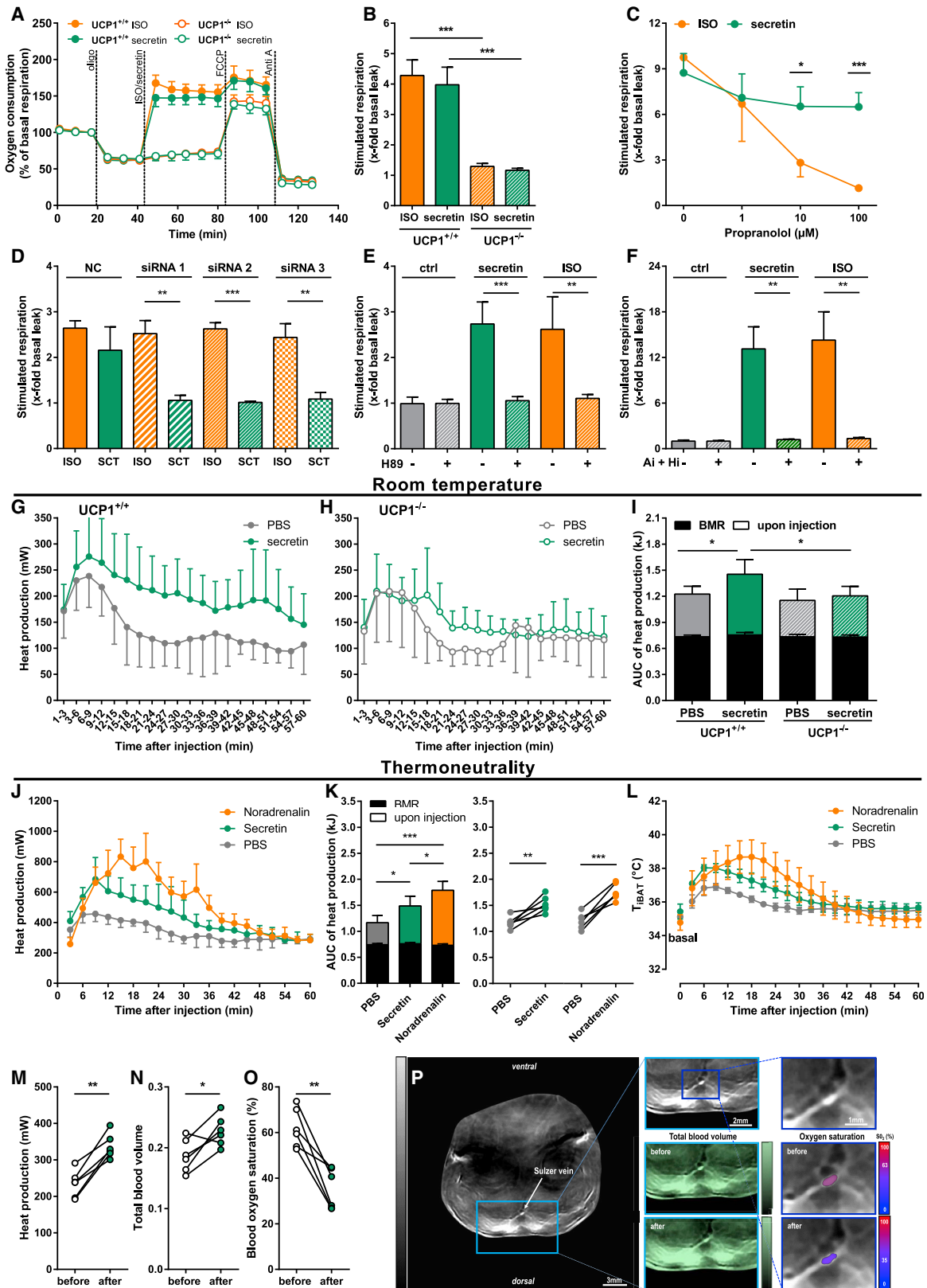
(F) Western blot analysis of SCTR, UCP1, and β -actin in both SVF and differentiated brown adipocytes. Data are presented as means \pm SD.

(B) Repeated-measures one-way ANOVA (Tukey's test), (C) one-way ANOVA (Tukey's test), (D) unpaired t test. * = $p < 0.05$, ** = $p < 0.01$, *** = $p < 0.001$. See also Figure S1.

The periprandial rise of secretin may suppress food consumption, as peripheral and central administration of secretin reduces food intake in fasted mice depending on the presence of the SCTR (Cheng et al., 2011). Integrated with our present finding, we hypothesized that secretin inhibits food intake through activation of BAT. To test this hypothesis, fasted mice were injected with 5 nmol secretin before refeeding. Secretin reduced food intake compared with PBS-injected mice (Figure 3C) during the first 2–3 hr of refeeding, possibly due to the short half-life of secretin (Curtis et al., 1976).

To further explore whether the reduction in food intake was dependent on BAT thermogenesis, we compared the effect of secretin on food intake in UCP1 WT and KO mice. Remarkably, the inhibitory effect of secretin on food intake was attenuated in UCP1-KO mice (Figures 3D and 3E). Therefore, we conclude that secretin-induced thermogenesis in BAT accelerates satiation

during the first bouts of refeeding. This satiation effect could be mediated either by direct activation of BAT or by central effects of secretin activating the sympathetic output to BAT. In contrast to the effect of β -3-AR agonist CL-316,243 (CL), the effects of secretin on food intake (Figures 3F–3H) and BAT temperature (Figures 3I–3P), however, were retained in mice pretreated with propranolol. Therefore, secretin directly activates BAT independent of the efferent sympathetic innervation. Consistent with previous findings (Grujic et al., 1997; Susulic et al., 1995), BAT activation by adrenergic signaling (CL) also leads to a suppression of appetite, which indicates that satiation is a general consequence of BAT thermogenesis. Moreover, our data also demonstrate that BAT plays a negligible role in pre-prandial thermogenesis (Figure S3A). While prandial thermogenesis and early postprandial thermogenesis do not depend on adrenergic signaling, as propranolol failed to block the increase



(legend on next page)

in BAT temperature induced by refeeding, late postprandial thermogenesis depends on adrenergic signaling (Figures S3A and S3B). This is consistent with the previous finding that the most pronounced effect of β -blockade on postprandial energy expenditure was found 3–4 hr after the meal (Astrup et al., 1989).

We next investigated the neurobiological basis of satiation induced by secretin-activated BAT. We found that secretin treatment elevated anorexigenic proopiomelanocortin (POMC) and repressed orexigenic agouti-related protein (AgRP) mRNA levels in the hypothalamus of fasted mice in an UCP1-dependent manner (Figures 3Q–3S). There was no effect of secretin on cocaine- and amphetamine-regulated transcript (CART) and neuropeptide Y (NPY) transcript levels (Figures S3C–S3E). Moreover, the expression of transient receptor potential vanilloid 1 (TRPV1), a temperature-sensitive ion channel expressed in POMC neurons, was upregulated by secretin treatment in the hypothalamus of WT but not in UCP1-KO mice (Figure 3T). Activation of TRPV1-like receptors in POMC neurons of the hypothalamic arcuate nucleus by warm temperature leads to appetite suppression (Jeong et al., 2018). Thus, our data support the idea that the TRPV1 receptor senses the rise in hypothalamic temperature due to BAT-mediated meal-associated prandial thermogenesis and activates the POMC neurons (Rampono and Reynolds, 1991). Congruently, we found that short-term heat exposure regulated neuropeptides and TRPV1 gene expression in a similar pattern as secretin treatment (Figures S3F and S3G). Together, these results suggest that the satiation signal emanating from secretin-activated BAT was sensed in the brain and promoted satiation, likely through perception of heat generated by BAT.

To further emphasize the strong relationship between BAT thermogenesis and food intake, we performed an analysis of around 2,000 food intake events in 23 mice during 70 hr (*ad*

libitum feeding) when BAT temperature was recorded simultaneously using implanted transmitters. Our analysis showed that (1) the initiation of feeding is always accompanied by a rise in iBAT temperature and that (2) the peak of iBAT temperature is followed by termination of feeding (Figures S3H–S3K). Therefore, a rise in iBAT temperature was plausibly the consequence of food intake and subsequently could have caused the termination of feeding. In short, thermogenic BAT plays an important role in the acute control of food intake in mice. Consistently, UCP1-KO mice showed dramatic alterations in feeding behavior with decreased number of meals, increased meal size and meal duration, and decreased inter-meal bout length, whereas total food intake was similar to WT mice (Figures 3U–3Z and S4). Taken together, secretin inhibits food intake through directly activating BAT thermogenesis and thereby conveys an unappreciated function of BAT in the control of satiation.

Neutralizing Prandial Secretin Activity Blunts Meal-Associated Thermogenesis, Increases Food Intake, and Changes Meal Patterning

Based on the thermogenic effects of exogenous secretin, we reasoned that endogenous release of secretin during refeeding stimulates prandial thermogenesis in BAT. A polyclonal secretin antibody was applied to neutralize the endogenous activity of secretin. This antibody completely neutralized purified secretin as well as endogenous blood-borne secretin mediated activation of SCTR signaling when tested *in vitro* (Figure S5). Refeeding of fasted mice was associated with an immediate rise in iBAT temperature by $\sim 2^\circ\text{C}$ within 30 min (Figure 4A). Compared to mice treated with isotype-like anti-GFP antibody, this rise in iBAT temperature was largely attenuated in mice pretreated with the secretin antibody (Figures 4A and 4B). The antibody also increased food intake during the early phase of refeeding

Figure 2. Secretin Activates UCP1-Dependent Thermogenesis Both *In Vitro* and *In Vivo*

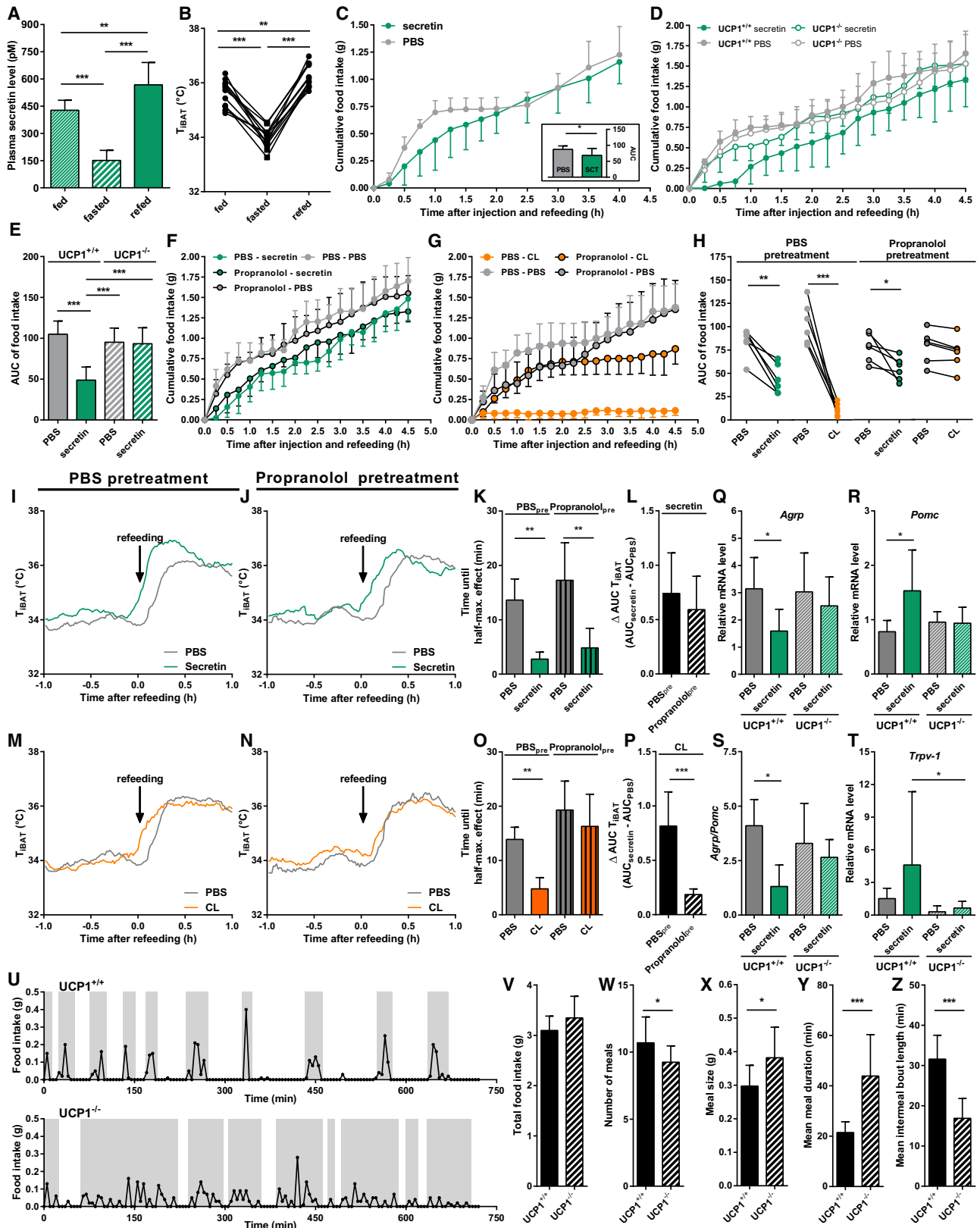
(A–F) Secretin activates UCP1-dependent thermogenesis through the SCTR-PKA-ATGL/HSL pathway in primary brown adipocytes. (A) Time course of oxygen consumption rate of UCP1 WT (UCP1^{+/+}) and KO (UCP1^{-/-}) brown adipocytes recorded by microplate-based respirometry (Seahorse XF96 Analyzer) under basal conditions and during successive addition of 5 μM oligomycin (oligo), 1 μM isoproterenol (ISO) or 10 nM secretin, 1 μM FCCP, and 5 μM antimycin A (Anti A). Data are expressed as percentage of basal respiration. (B) Quantitation of ISO- and secretin-stimulated UCP1-mediated uncoupled respiration in UCP1^{+/+} and UCP1^{-/-} brown adipocytes. Data are expressed as fold of basal leak respiration, 1-fold of basal leak indicating no stimulation of UCP1-mediated uncoupled respiration (n = 5). (C) Effects of various concentrations of propranolol, a non-selective blocker of β -adrenergic receptors, on secretin- and ISO-stimulated UCP1-mediated uncoupled respiration in brown adipocytes (n = 3). (D) SCT (secretin)- and ISO-stimulated respiration in primary brown adipocytes after siRNA-mediated knockdown of the secretin receptors in comparison to a non-targeting control (NC) (n = 3). (E) UCP1-mediated uncoupled respiration expressed as fold increase of basal leak respiration after stimulation with ISO, secretin, and vehicle (assay medium) without protein kinase A inhibitor H89 (50 μM), which was injected together with oligo prior to addition of stimulators (n = 3). (F) Respiration stimulated by ISO, secretin, or vehicle as fold increase of basal leak after 1 hr pre-treatment with both 40 μM A_i (Atglistatin, ATGL-inhibitor) and H_i (Hi76-0079, HSL-inhibitor) (n = 4).

(G–I) The thermogenic effect of secretin in UCP1^{+/+} (G) and UCP1^{-/-} (H) mice kept at room temperature. After determining the basal metabolic rate (BMR) at 30°C, respiration of mice treated with either 5 nmol secretin or equal volume PBS via intraperitoneal injection (i.p.) was measured by indirect calorimetry for 1 hr at 27°C. BMR and heat production upon stimulation were quantified as area under the curve (AUC) (I) (n = 6–9).

(J–L) The thermogenic effects of secretin (5 nmol), noradrenalin (1 mg/kg), and PBS on mice acclimatized for 1 week to thermoneutrality (30°C). Heat production was determined by the same procedure as for mice kept at room temperature. Additionally, the temperature of interscapular brown adipose tissue was recorded via implanted E-mitter (L).

(M–P) Direct visualization of BAT activation by secretin (5 nmol) in nude mice through indirect calorimetry coupled with multispectral optoacoustic tomography (MSOT) (n = 6). (M) Heat production before and after intravenous secretin injection (5 nmol). (N) Normalized MSOT image signal of total blood volume (TBV) in the Sulzer vein (SV) before and after intravenous (i.v.) injection of secretin. (O) Oxygen saturation (SO₂) calculated as MSOT signal ratio between oxygenated hemoglobin and TBV in the SV before and after i.v. injection of secretin. (P) Representative reconstructed anatomical MSOT image (800 nm) showing iBAT and the Sulzer vein *in vivo* in three different magnifications as well as TBV (green) and SO₂ (red/blue) before and after i.v. secretin injection. Data are presented as means \pm SD or individual values.

(B, C, and I) Two-way ANOVA (Tukey's test), (D–F) unpaired t test, (M–O) paired t test. * = p < 0.05, ** = p < 0.01, *** = p < 0.001. See also Figure S2.



(legend on next page)

(Figures 4C–4E). Detailed analysis revealed a negative correlation between the rise in iBAT temperature and food intake (Figure 4F). Thus, secretin released endogenously in response to food intake is a physiological mediator of meal-associated thermogenesis in BAT, and the induction of BAT thermogenesis is necessary for the inhibitory effect of secretin on food intake. Our findings demonstrate a novel endocrine gut-secretin-BAT-brain axis in the acute control of food intake.

Analyzing the feeding behavior of WT mice treated with the secretin antibody under *ad libitum* feeding conditions, we found that these WT mice phenocopied the UCP1-KO mice by showing increased meal sizes as well as longer meal durations (Figures 4G–4K). Therefore, disruption of the gut-BAT-brain axis in the control of satiety by blocking endogenous secretin activity alters feeding behavior. We thereby recapitulate our findings in a WT mouse model with acute loss of secretin function that is not subject to long-term adaptive responses due to genetic ablation as may be prevalent in germline UCP1-KO.

Secretin Infusion Transiently Elevates Energy Expenditure in Diet-Induced Obese Mice

Secretin promoted negative energy balance through both increasing energy expenditure and decreasing energy intake and therefore may hold promise for developing novel obesity therapies. To clarify the potential therapeutic uses, we chronically infused diet-induced obese mice (DIO) with native human secretin (native secretin) and a modified human secretin analog (modified secretin), respectively. In a first experiment conducted with DIO mice kept at room temperature (RT), the modified secretin caused a small transient reduction in cumulative food intake (Figure S6A) and body weight gain (Figure S6B). After 2 weeks of treatment, body fat mass was slightly lower in modified-secretin-treated mice. This was not reflected by a lower body mass as the lean mass was slightly increased in these mice (Figure S6C). Compared to GLP-1 as a positive control,

these effects were minor. Employing a linear mixed effects model to test whether secretin also affects metabolic rate, we found that the small effect of secretin on food intake was not alone explained by the starting body weight (which captures the metabolic requirements of the animal) and the change in body weight (which primarily captures the alternate fate of food: fat deposition loss), suggesting that the modified secretin modulated metabolic rate.

Effects on energy expenditure at RT may be masked, as this thermal environment already imposes a cold challenge on mice and activates thermoregulatory heat production, mainly in BAT, as exemplified by a nearly 2-fold increase of resting metabolic rate by transfer from 30°C to 20°C (Fischer et al., 2018). Therefore, we conducted a second experiment to directly measure whether chronic infusion of the modified secretin increases energy expenditure analyzed as heat production in DIO mice kept at TN. On days 1 and 2 after start of infusion, the modified secretin led to a transient increase in daily energy expenditure by 32% and 9%, respectively (Figures 5A–5C). No such effect on energy expenditure was observed in control mice infused with native secretin, or with the GLP-1 analog. The GLP-1 analog induced a pronounced decrease in food intake and body fatness, whereas the minor effects of the modified secretin on body composition observed at RT were not observed at TN (Figures 5D–5F). We conclude that the transient increase in energy expenditure after onset of chronic infusion of the human secretin analog strongly promoted negative energy balance in DIO mice even when kept at TN. Notably, mice infused with the modified secretin at TN showed a significant increase in water intake most likely to compensate for increased water secretion by the pancreas (Figure 5G).

These data demonstrate thermogenic activity of secretin also in DIO mice but rather discourage the application of chronically elevated secretin levels as a therapeutic option for the treatment of obesity.

Figure 3. Secretin Inhibits Food Intake through Direct Activation of BAT Thermogenesis in Mice

- (A) Plasma secretin levels of mice fed *ad libitum*, fasted for 18 hr, and/or refed for 1 hr after 17 hr of fasting (n = 6).
 (B) Temperature of iBAT (T_{iBAT}) of fed, fasted, and refed mice. T_{iBAT} was calculated as mean of 1 hr period (fed: random 1 hr; fasted: 1 hr before refeeding; refed: 1 hr after refeeding) (n = 12).
 (C) Cumulative food intake of overnight fasted (18 hr) C57BL6/N mice upon refeeding. Mice were injected (i.p.) with either secretin or vehicle (PBS) before refeeding. For statistics, we calculated area under cumulative food intake–time curve (see inset: AUC 0–2.5 hr) (n = 11–12).
 (D) The effects of secretin on acute food intake in overnight fasted (18 hr) UCP1^{+/+} and UCP1^{-/-} 129S1/SvEv mice upon refeeding.
 (E) The area under cumulative food intake–time curve (AUC 0–2.5 hr) was calculated (n = 6).
 (F–H) The effects of β -blocker propranolol (10 mg/kg BW) pre-treatment (20 min prior to secretin, CL, or PBS injection) on secretin (5 nmol) (F) and CL 316,243 (CL, 1 mg/kg BW) (G) induced suppression of food intake in overnight (18 hr) fasted 129S6/SvEv mice, respectively. (H) Area under cumulative food intake curve (AUC 0–2.5 hr) was quantified (n = 6).
 (I–P) The effects of β -blocker propranolol (10 mg/kg BW) pre-treatment (20 min prior to secretin, CL, or PBS injection) on refeeding-induced rise in iBAT temperature in overnight (18 hr) fasted mice without secretin and CL treatments. Propranolol delayed the rise of CL-induced T_{iBAT} but not refeeding- or secretin-induced T_{iBAT} as quantified by the required time to reach half-maximal iBAT temperature in response to refeeding/injection (K and O) as well as the calculated differences between the AUC of secretin- (L) or CL-induced (P) rise in iBAT temperature and their corresponding PBS controls (Δ AUC T_{iBAT}) under both PBS and propranolol pre-treatment conditions.
 (Q–T) The neurobiological basis of satiety induced by secretin-activated BAT. Relative expression abundance of *Agpr* (agouti-related protein) (Q), *Pomc* (pro-opiomelanocortin) (R), and *Trpv-1* (transient receptor potential vanilloid 1) (T) in hypothalamus of fasted UCP1^{+/+} and UCP1^{-/-} mice in response to i.p. injection of PBS or secretin (hypothalamus was removed 4 hr after injection). (S) Ratio of *Agpr* and *Pomc* expression.
 (U–Z) Feeding patterns of UCP1^{+/+} and UCP1^{-/-} 129S1/SvEv mice. (U) Representative food intake of one UCP1^{+/+} and one UCP1^{-/-} mouse during dark phase. Meals defined as food intake >0.005 g; inter-meal bout lengths \geq 15 min are indicated in gray. Total food intake (V), number of meals (W), mean meal size (X), mean meal duration (Y), and mean inter-meal bout length (Z) during dark phase (n = 12) were quantified.
 (A) One-way ANOVA (Tukey's test), (B) RM one-way ANOVA, (C, L, P–T, V, and X–Z) unpaired t test, (H, K, and O) paired t test, (E) two-way ANOVA (Tukey's test), (W) non-parametric t test as normality test failed. Data are presented as means \pm SD. * = p < 0.05, ** = p < 0.01, *** = p < 0.001. See also Figures S3 and S4.

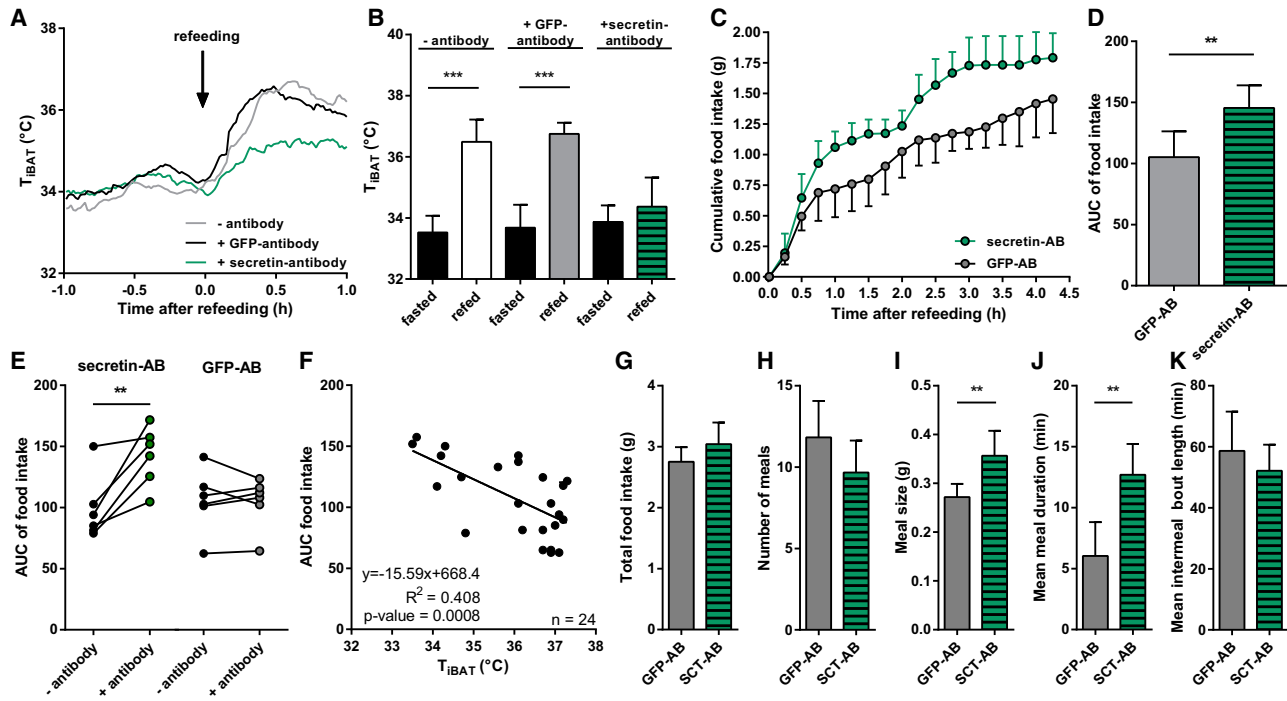


Figure 4. Neutralization of Endogenous Secretin Prevents Meal-Induced Increase in iBAT Temperature and Acutely Increases Food Intake

(A–F) Refeeding responses, in terms of rise in T_{iBAT} and increase in cumulative food intake, were recorded (1-min bins) in overnight fasted mice (18 hr) upon refeeding under control, GFP-antibody-, and secretin-antibody-treated conditions. In total, 12 mice were used for non-treated control characterization. After 1 week washout to minimize the potential previous effects of fasting, mice were divided into two groups ($n = 6$) and either injected with GFP or secretin antibody when fasted again. (A) Time course changes of T_{iBAT} in secretin-antibody-injected mice in comparison with GFP-antibody- and non-treated controls upon refeeding. (B) Minimal and maximal T_{iBAT} of control, GFP-, and secretin-antibody-injected mice compared to respective controls within 30 min before and 30 min after refeeding. (C) Cumulative food intake of mice pre-treated with GFP- or secretin-antibody within 4.5 hr of refeeding. (D) The area under cumulative food intake–time curve (AUC 0–2.5 hr) was calculated. (E) Paired comparison of individual AUC_{0–2.5 hr} of food intake before and after antibody treatment. (F) Negative correlation of AUC_{0–2.5 hr} of food intake and iBAT temperature.

(G–K) Feeding behavior of *ad libitum*-fed mice treated with either secretin antibody of GFP antibody. Total food intake (G), number of meals (H), mean meal size (I), mean meal duration (J), and mean inter-meal bout length (K) of GFP- or secretin-antibody-treated 129S6/SvEv mice during one dark phase. The analysis was performed 2 days after the antibody injection to minimize previous fasting effects ($n = 6$).

Data are presented as means \pm SD or individual values. (D and G–K) Unpaired t test, (B and E) paired t test. * = $p < 0.05$, ** = $p < 0.01$, *** = $p < 0.001$. See also Figure S5.

Secretin Activates Human BAT

We addressed the biological significance of thermogenic action of secretin in humans. For this purpose, secretin concentrations were measured in serum samples from human subjects showing BAT activation in response to a single meal, as reported very recently (U Din et al., 2018). Consistent with our observations in mice, serum secretin levels increased after single-meal ingestion (Figure 6A). The increment of plasma secretin levels induced by a single meal positively correlated with postprandial oxygen consumption rates and fatty acid uptake rates in BAT (Figures 6B and 6C). Direct evidence for the thermogenic action of secretin in BAT was obtained by FDG-PET-CT scans after two secretin infusions that significantly increased serum secretin level (Figure S6D) and glucose uptake in human BAT compared to placebo control treatment (Figure 6D). Collectively, we propose that the satiation axis sparked by BAT activation through secretin is conserved from mouse to man.

DISCUSSION

Thermogenesis in brown adipose tissue, contributing to meal-associated thermogenesis (or diet-induced thermogenesis) and cold-induced non-shivering thermogenesis, is generally believed to be switched on by noradrenaline released from sympathetic nerve endings. In this study, we identified that the gut hormone secretin, upon release during eating, serves as a novel non-sympathetic BAT activator mediating prandial thermogenesis, which consequentially induces satiation. We thereby reveal a gut-secretin-BAT-brain axis in mammals that constitutes the physiological basis of prandial thermogenesis in the control of satiation. Establishing a largely unappreciated function of BAT in the control of hunger and satiation qualifies BAT as an even more attractive target for treating obesity. Demonstration of a non-canonical gut-secretin-BAT-brain axis beyond the canonical gut-brain-BAT axis uncovers

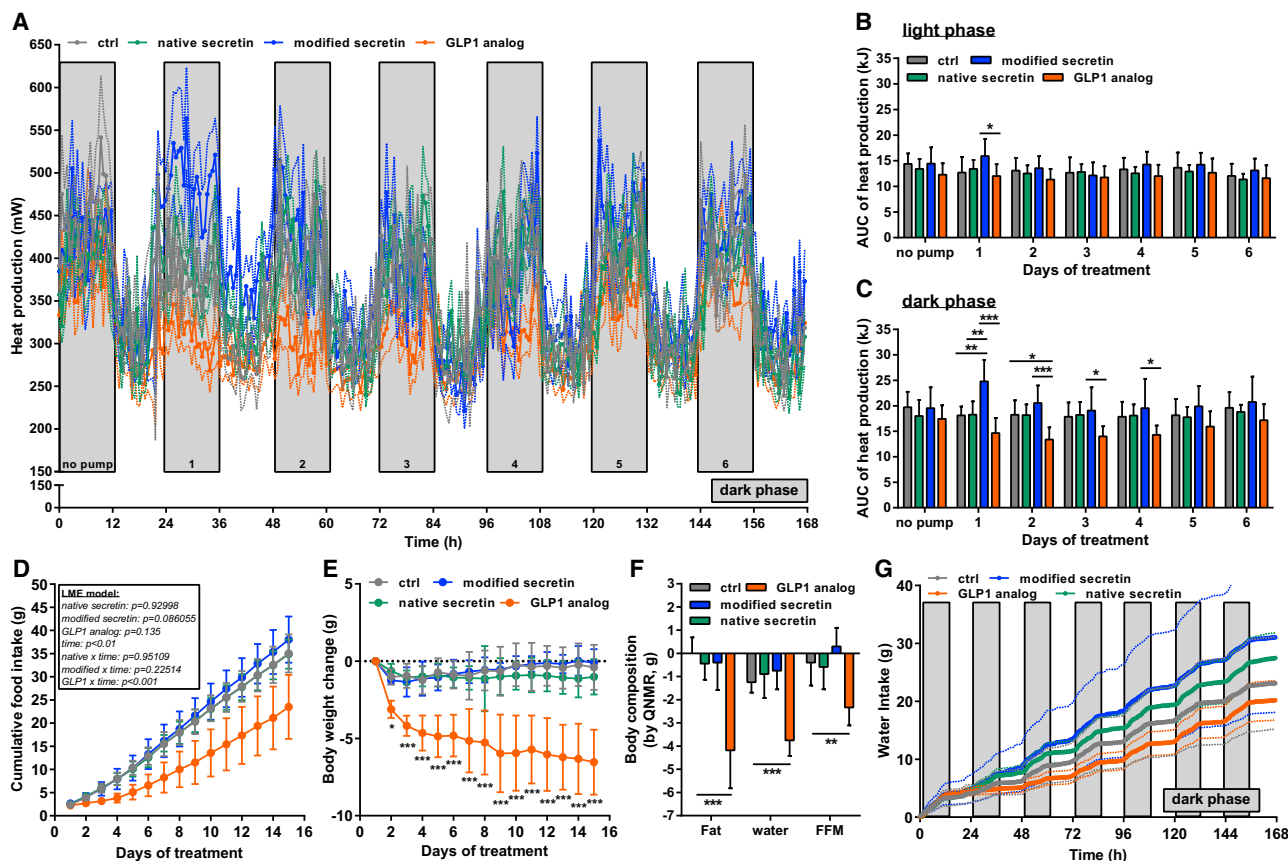


Figure 5. Secretin Infusion Transiently Increases Energy Expenditure in Diet-Induced Obese Mice at Thermoneutrality

(A–G) The effects of continuous infusion of native secretin (996 nmol/kg/day), modified secretin (326 nmol/kg/day), GLP1 analog (CEX51, 30 nmol/kg/day), or vehicle (20 mM Citrate) on metabolic parameters such as heat production (A–C), cumulative food intake (D), body weight changes (E), and changes in body composition from day 1 to day 14 (F) as well as water intake (G) in diet-induced obese (DIO) male C57BL6/N mice kept at thermoneutrality (30°C). The continuous infusion with subcutaneous miniosmotic-pumps (12 μ l/mouse/day) lasted 2 weeks. Heat production data was only presented for the first 6 days as no differences were observed in the second experimental week. Area under the heat production time curve was calculated for light (B) and dark (C) phases separately. Dashed lines in (A) and (G) represent standard deviation of corresponding groups. (D) Linear mixed effects model with “treatment,” “time” and their interaction as fixed effects, and “individual” as random factor. (F) One-way ANOVA (Tukey’s test), (B, C, and E): repeated-measures two-way ANOVA (Tukey’s test). * = $p < 0.05$; ** = $p < 0.01$, *** = $p < 0.001$. See also Figure S6.

a yet unknown facet of the complex regulatory system controlling energy balance.

Secretin, an Old Dog Playing a New Trick

Secretin was the first hormone discovered and laid grounds for the conceptual framework of endocrine regulation (Bayliss and Starling, 1902). It stimulates water and bicarbonate secretion from pancreas to ensure a proper milieu for digestion and absorption of macronutrients and inhibits gastric emptying. Beyond these well-characterized gastrointestinal functions, secretin exhibits metabolic control functions, such as stimulation of lipolysis in white adipocytes (Sekar and Chow, 2014b) and inhibition of food intake (Cheng et al., 2011). The latter anorexigenic action of secretin was reported to depend on the activation of secretin receptors in vagal sensory nerves and melanocortin signaling in the brain (Cheng et al., 2011; Chu et al., 2013). Our study demonstrates that secretin, upon

release during eating, directly activates BAT thermogenesis. Secretin executes this thermogenic action by signaling via secretin receptors abundantly expressed in brown adipocytes. The BAT activation function of secretin is conserved in human. This BAT activation by secretin is essential for the acute satiating effect of secretin. This link between secretin-induced BAT thermogenesis and satiation is underlined by the observed negative correlation of food intake and meal-associated rise in iBAT temperature. We thereby assign a new metabolic control function to secretin as an endocrine activator of prandial thermogenesis in BAT. We propose that the nutritional status encoded by the meal-induced rise in blood secretin levels is directly transformed into thermogenic activity of BAT, which relays this information to the brain and promotes satiation. This establishes a yet unknown endocrine gut-secretin-BAT-brain axis with major implications for integrative energy balance physiology.

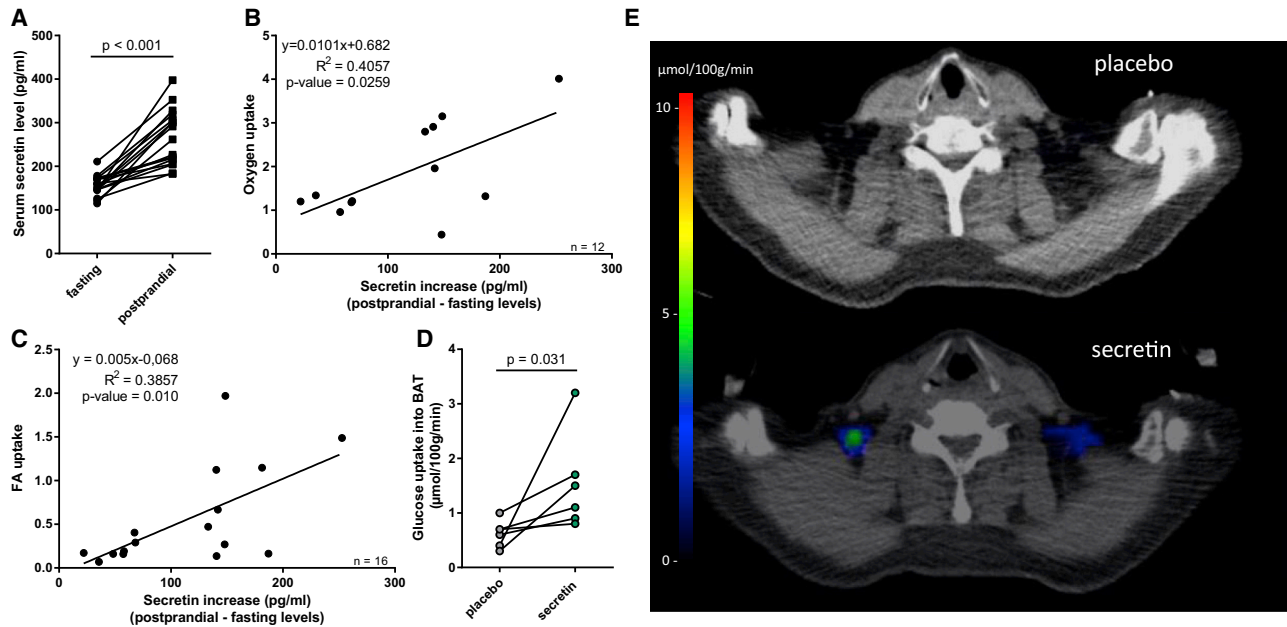


Figure 6. Secretin Increases Glucose Uptake in Human BAT

(A–C) Serum secretin level upon a single meal ingestion in humans ($n = 17$). Correlation upon meal ingestion of serum secretin levels and postprandial oxygen (B) and fatty acid uptake (C) in BAT, respectively.

(D) Effect of secretin infusion on glucose uptake in human BAT compared to placebo ($n = 6$).

(E) Representative parametric PET-CT image from supraclavicular BAT areas showing increased glucose uptake after secretin infusion.

(A) Parametric paired t test, (D) non-parametric paired t test. See also Figure S6.

Secretin as an Endocrine Mediator of Meal-Associated Thermogenesis

Meal-associated thermogenesis consists of two parts, the obligatory metabolic costs of food handling for ingestion, digestion and absorption (handling thermogenesis) and facultative thermogenesis. The existence of the latter is still debated, including source of thermogenesis (BAT dependent or not), functional significance and potential mediators (Cannon and Nedergaard, 2004; Kozak, 2010). BAT as a heater organ has been suggested as a source for facultative meal-associated thermogenesis (Cannon and Nedergaard, 2004; Kozak, 2010). The general concept of a gut – brain – BAT axis consisted of gastrointestinal hormones being sensed in the brain, either directly or via neural afferent projections increase SNS activity, and stimulate meal-associated thermogenesis by release of norepinephrine in BAT (Bachman et al., 2002). A contribution of such postprandial sympathetic activation to meal-associated thermogenesis is not always evident (Welle et al., 1981). Notably, β -blockade failed to reduce metabolic rate in man during the first 3 hours after a carbohydrate meal (Zwilling et al., 1981) or mixed meal (Thörne and Wahren, 1989), but exerted a significant effect in the period 3–4 hours after the meal (Astrup et al., 1989). It thus appears that while sympathetically mediated thermogenesis in the late postprandial phase cannot be ruled out, the prandial and early postprandial rise in energy expenditure is initiated by mechanisms independent of the SNS. Consistent with this notion, we found that secretin, as a non-sympathetic endocrine activator, mediates prandial thermogenesis, which may explain the non-sympa-

thetically mediated meal-associated thermogenesis. In contrast to previous studies, focused on postprandial thermogenesis or diet-induced thermogenesis mediated by the SNS activation in animals exposed to long term cafeteria/high-fat diets, we here examined the prandial rise in thermogenesis by directly monitoring iBAT temperature. This physiological readout is unbiased by the animal activity as observed by indirect calorimetry. Recording BAT temperature demonstrated that onset of refeeding acutely activated BAT thermogenesis and this acute prandial BAT thermogenesis is largely independent of adrenergic signaling. Therefore, our study revealed a previously unappreciated BAT – derived thermogenesis during the prandial phase that functions as a signal to the brain to terminate a meal.

Secretin-Activated Brown Fat Controls Food Intake

Our findings elucidate a novel molecular mechanism for meal-associated thermogenesis with BAT acting as a peripheral communication hub between the gut and the brain. In a physiological context, one may question why BAT dissipates part of the energy ingested during a meal where no extra heat production is necessary for body-temperature regulation. Integrating thermostatic (Brobeck, 1948) and glucostatic (Mayer, 1953) hypotheses, meal-associated thermogenesis in BAT was suggested to play a key role in thermoregulatory feeding (Himms-Hagen, 1995). However, this concept was not further pursued mostly because the loss of thermogenic function in BAT does not cause hyperphagia in UCP1-KO mice, and the β -blocker propranolol does not increase meal sizes (Cannon and Nedergaard, 2004).

We here reveal that secretin-induced satiation in fasted mice during refeeding depends on the presence of UCP1 and thus on thermogenic BAT function. If BAT relays information on nutritional status to the brain, we suggest that the meal-associated wasting of nutrient energy in BAT, beyond its role in buffering the overwhelming caloric load during feeding, is an inevitable result of this relay function (the cost of a signal). We therefore propose a physiological function of secretin-mediated prandial thermogenesis in the control of satiation. Further evidence compatible with this proposal is provided by our observation that systemic blockade of secretin function not only attenuated the prandial rise in iBAT temperature but also increased food intake. The effect of secretin on thermogenesis and food intake were absent in UCP1-KO mice. In addition, these mice showed a drastic alteration in meal patterning, with longer bouts of feeding indicating a delayed perception of satiation compared to WT mice. These findings consolidate the existence of a gut-secretin-BAT-brain axis involved in the regulation of satiation. Similar to UCP1-KO mice, secretin and SCTR germline KO mice are not hyperphagic but display normal body weight and food intake (Cheng et al., 2011; Sekar and Chow, 2014a). Disruption of the proposed gut-secretin-BAT-brain axis in the control of satiation is apparently compensated by other anorexigenic pathways preventing long-term disturbances of energy balance, as exemplified by the mild metabolic phenotypes (eat normally and maintain the same body weight as WT mice) of several gut hormone and gut hormone receptor KO mice, such as ghrelin KO mice, CCK and its receptor KO mice, and GLP-1 and its receptor KO mice, highlighting the extensive compensatory mechanisms occurring *in vivo* (see review in Strader and Woods [2005]). However, meal patterning, which is altered in UCP1-KO mice, has not been studied in secretin- and SCTR-deficient mouse models so far. It is highly likely that these germline KO mouse models compensate for increased meal size by initiating fewer meals and thereby maintain body weight due to the interaction between long-term energy homeostasis and meal-related satiation signals. In this scenario, tissue-specific ablation of UCP1, secretin, and SCTR in the adult stage is required to further explore our hypothesis.

Brown Fat Relays Nutritional Status to the Brain

Gut hormones play a critical role in relaying signals of nutritional and energy status from the gut to the central nervous system in order to regulate food intake. Canonically, satiation signals reach the brain either directly via the blood (e.g., amylin and ghrelin) or indirectly by activation of vagal afferent nerves in the intestine (e.g., CCK and GLP-1). In our study, the common satiating effect evoked by secretin and CL indicates that meal termination by BAT-derived heat production is another alternative general mechanism. The hypothalamus and brainstem harbor metabolic sensors, which play a central role in the control of hunger and satiation. Therefore, the meal-termination signal that encodes the nutritional status must be relayed from BAT to the brain. Consistent with this notion, secretin treatment increases anorectic neuropeptide expression in hypothalamic nuclei (Cheng et al., 2011). Our study further demonstrated that the modulatory effects of secretin on feeding-related neuropeptides were UCP1 dependent, consolidating the essential role of BAT

thermogenesis in mediating the satiation effect of secretin. Regarding communication between BAT and said brain regions, it is most likely that a rise in local brain temperature caused by BAT thermogenesis represents the key signal inducing satiation. This view is supported by a classical study demonstrating a rise in temperature in the preoptic hypothalamic area during feeding in rats, where a strong positive correlation was found between the maximal temperature rise in the hypothalamus and the duration of feeding (Abrams and Hammel, 1964). And there is further evidence that BAT thermogenesis contributes to increases in body and brain temperature under *ad libitum* condition (Blessing et al., 2013). A very recent report found a subpopulation of POMC neurons expressing the temperature-sensitive ion channel, TRPV1, which can directly sense local changes in brain temperature. Slight increases in body temperature in response to exercise caused a TRPV1-dependent increase in the activity of POMC neurons, which suppressed feeding in mice (Jeong et al., 2018). Consistent with this scenario, we discovered that secretin treatment altered *Trpv1* transcript abundance in the hypothalamus of WT but not UCP1-KO mice. Despite our data indicating heat as a signal, other possibilities such as neuronal or endocrine mechanisms cannot be excluded. Secretin-induced release of adipokines (batokines) or neuronal afferent signaling may alter melanocortin signaling in the hypothalamus. In fact, it has been postulated that afferent sensory nerves in BAT sense the thermal status, blood flow, or intracellular lipolytic products and hence regulate BAT thermogenesis via efferent SNS output (Bartness et al., 2010). Of note, several hypothalamic nuclei such as the paraventricular nucleus, dorsomedial hypothalamus, and lateral hypothalamus receive sensory inputs from fat depots, pointing toward a sensory feedback mechanism (Ryu et al., 2015). This alternative or complementary pathway of BAT-brain communication along the gut-secretin-BAT-brain axis is supported by the observation that the anorexigenic action of secretin depends on afferent sensory nerves (Chu et al., 2013). Further studies are warranted to dissect the contributions of these potential mechanisms. In any case, demonstration of a non-canonical role of BAT in relaying nutritional status to brain beyond the canonical gut-vagal nerve-brain axis uncovers a yet unknown facet of the complex regulatory system that contributes to the termination of feeding.

Meal-Related Satiation Signal and Long-Term Adiposity

Despite the ability of some gastrointestinal hormones such as CCK in previous studies and secretin in our study to reliably reduce meal size when administered prior to a meal, their repeated administration is largely ineffective in reducing food intake and body weight, mainly due to increased feeding frequency to compensate for the suppressed meal size. Thus, orchestration of gut-derived satiation and satiety signals contributes to the maintenance of a relatively constant level of body fat/weight, possibly through interaction with long-term adiposity-related signals (leptin and insulin). This accounted for the negligible effect of chronic secretin infusion to suppress body weight as compared to the pronounced effect of a GLP1 analog with its dual function of both satiation and satiety signal. Indeed, suppression of food intake induced by the GLP-1 analog arises from a combination of reduced meal size and

increased inter-meal interval (Williams et al., 2009). In murine model systems with *ad libitum* access to food, gut-hormone-based therapies require targeting both satiation and satiety in an effort to alter energy homeostasis. In a setting closer resembling the human meal pattern, however (i.e., three 30-min meals per day), laboratory rats could not compensate for the satiating effect of the peptide and consequently lost weight (West et al., 1982). Presence or absence of an altered systemic energy balance thus remains to be determined in man.

Together, these data demonstrate secretin-activated brown fat to be a hub for satiation signaling to reduce meal size and initiate meal termination. Brown adipose tissue thermogenesis thus constitutes a unique target mechanism to manipulate both energy expenditure and energy intake.

Future Perspectives

Research addressing the (patho-) physiological relevance of BAT is concentrating on thermogenesis and the capacity to increase resting metabolic rate. Based on the results of our study, however, the view of BAT as a mere catabolic heater organ must be revised, and more attention needs to be directed toward the function of BAT in the control of hunger and satiation. Several reports demonstrated that glucose and fatty acid uptake in BAT is increased in rodents and humans exposed to a single meal and that maximal thermogenesis coincides with meal termination (Blessing et al., 2013; Glick et al., 1981; U Din et al., 2018; Vosselman et al., 2013), but there has been a lack of experimental proof for a role of BAT thermogenesis in the control of food intake. According to our data, any stimulus that activates BAT thermogenesis could potentially induce satiation. Targeting this mechanism by nutritional or pharmacological interventions such as enforcing or stimulating the transient meal-associated surge of secretin secretion may provide novel treatment options. In conclusion, we demonstrate that BAT regulates energy intake. Activation of the gut-BAT-brain axis not only increases energy expenditure but also promotes satiation, therefore qualifying this physiological mechanism as an attractive, peripheral target for the treatment of obesity.

STAR★METHODS

Detailed methods are provided in the online version of this paper and include the following:

- [KEY RESOURCES TABLE](#)
- [CONTACT FOR REAGENT AND RESOURCE SHARING](#)
- [EXPERIMENTAL MODEL AND SUBJECT DETAILS](#)
 - Animals
 - Primary cell culture
 - Human study
- [METHOD DETAILS](#)
 - RNA-sequencing
 - Western Blot
 - Gene expression analysis (qRT-PCR)
 - Respiration assays
 - Surgical implantation of telemetry transmitters
 - Monitoring of food intake and iBAT temperature
 - Indirect calorimetry

- Macroscopic multi-spectral optoacoustic tomography (MSOT) combined with indirect calorimetry
- Analysis of food intake data
- Measurement of plasma secretin concentrations
- Hypothalamic neuropeptides gene expression analysis
- Diet-induced obese mice study
- Dual luciferase reporter assay
- [QUANTIFICATION AND STATISTICAL ANALYSIS](#)
- [DATA AND SOFTWARE AVAILABILITY](#)

SUPPLEMENTAL INFORMATION

Supplemental Information includes six figures and can be found with this article online at <https://doi.org/10.1016/j.cell.2018.10.016>.

ACKNOWLEDGMENTS

This work was supported by grants to M.K. from the Deutsche Forschungsgemeinschaft (DFG) (KL973/11&12 and RTG1482) and the Else Kröner-Fresenius-Stiftung. K.S. and S.-M.G. were fellows in the DFG Research Training Group RTG1482. V.N. was funded by the DFG (Leibniz Prize 2013; NT 3/10-1) and the European Research Council (grant agreement 694968). PET studies were conducted at the Finnish CoE in Cardiovascular and Metabolic Diseases with support from Academy of Finland (259926, 265204, 292839, and 269977), University of Turku, Turku University Hospital, Åbo Akademi University, and European Union (EU FP7 project 278373; DIABAT). Thanks to Sabine Mocek (TUM), Uwe Klemm (IBM), and Sarah Glasl (IBM) for excellent technical assistance and Gael Diot for advice on data analysis. The images used for graphical abstract construction were purchased from Fotolia (© benchart, Alexander Pokusay, yuchy/Fotolia.com).

AUTHOR CONTRIBUTIONS

Y.L. and K.S. contributed equally to this study. Y.L., K.S., F.B., and M.K. conceived and designed the study. Y.L. found UCP1 activation property of secretin and provided key visions of the study. K.S. established methods. K.S., S.-M.G., A.B.-H., and Y.L. performed experiments. K.S. analyzed data. M.W., J.R., A.K., and V.N. performed the MSOT analysis. S.L., M.L., M.D., K.A.V., and P.N. performed the human experiments. T.C., L.S.O., and J.A.-F. performed the DIO experiments. T.F. provided the RNA-seq data and helped with MATLAB analysis. Y.L., K.S., and M.K. wrote the manuscript. All authors read and approved the manuscript.

DECLARATION OF INTERESTS

The Technical University of Munich has applied for a patent. T.C., L.S.O., and J.A.-F. were employees from Eli Lilly and Company.

Received: March 14, 2018

Revised: August 6, 2018

Accepted: October 2, 2018

Published: November 15, 2018

REFERENCES

- Abrams, R., and Hammel, H.T. (1964). Hypothalamic temperature in unanesthetized albino rats during feeding and sleeping. *Am. J. Physiol.* 206, 641–646.
- Afroze, S., Meng, F., Jensen, K., McDaniel, K., Rahal, K., Onori, P., Gaudio, E., Alpini, G., and Glaser, S.S. (2013). The physiological roles of secretin and its receptor. *Ann. Transl. Med.* 1, 29.
- Astrup, A., Simonsen, L., Bülow, J., Madsen, J., and Christensen, N.J. (1989). Epinephrine mediates facultative carbohydrate-induced thermogenesis in human skeletal muscle. *Am. J. Physiol.* 257, E340–E345.

- Bachman, E.S., Dhillon, H., Zhang, C.Y., Cinti, S., Bianco, A.C., Kobilka, B.K., and Lowell, B.B. (2002). betaAR signaling required for diet-induced thermogenesis and obesity resistance. *Science* 297, 843–845.
- Bartness, T.J., Vaughan, C.H., and Song, C.K. (2010). Sympathetic and sensory innervation of brown adipose tissue. *Int. J. Obes.* 34 (Suppl 1), S36–S42.
- Bayliss, W.M., and Starling, E.H. (1902). The mechanism of pancreatic secretion. *J. Physiol.* 28, 325–353.
- Beiroa, D., Imbernon, M., Gallego, R., Senra, A., Herranz, D., Villarroya, F., Serrano, M., Ferno, J., Salvador, J., Escalada, J., et al. (2014). GLP-1 agonism stimulates brown adipose tissue thermogenesis and browning through hypothalamic AMPK. *Diabetes* 63, 3346–3358.
- Berbée, J.F., Boon, M.R., Khedoe, P.P., Bartelt, A., Schlein, C., Worthmann, A., Kooijman, S., Hoeke, G., Mol, I.M., John, C., et al. (2015). Brown fat activation reduces hypercholesterolaemia and protects from atherosclerosis development. *Nat. Commun.* 6, 6356.
- Blessing, W., Mohammed, M., and Ootsuka, Y. (2013). Brown adipose tissue thermogenesis, the basic rest-activity cycle, meal initiation, and bodily homeostasis in rats. *Physiol. Behav.* 121, 61–69.
- Blondin, D.P., Daoud, A., Taylor, T., Tengelstad, H.C., Bézaire, V., Richard, D., Carpentier, A.C., Taylor, A.W., Harper, M.E., Aguer, C., and Haman, F. (2017). Four-week cold acclimation in adult humans shifts uncoupling thermogenesis from skeletal muscles to brown adipose tissue. *J. Physiol.* 595, 2099–2113.
- Blondin, D.P., Labbé, S.M., Tengelstad, H.C., Noll, C., Kunach, M., Phoenix, S., Guérin, B., Turcotte, E.E., Carpentier, A.C., Richard, D., and Haman, F. (2014). Increased brown adipose tissue oxidative capacity in cold-acclimated humans. *J. Clin. Endocrinol. Metab.* 99, E438–E446.
- Blouet, C., and Schwartz, G.J. (2012). Duodenal lipid sensing activates vagal afferents to regulate non-shivering brown fat thermogenesis in rats. *PLoS ONE* 7, e51898.
- Braun, K., Oeckl, J., Westermeier, J., Li, Y., and Klingenspor, M. (2018). Non-adrenergic control of lipolysis and thermogenesis in adipose tissues. *J. Exp. Biol.* 221. <https://doi.org/10.1242/jeb165381>.
- Brobeck, J.R. (1948). Food intake as a mechanism of temperature regulation. *Yale J. Biol. Med.* 20, 545–552.
- Cannon, B., and Nedergaard, J. (2004). Brown adipose tissue: function and physiological significance. *Physiol. Rev.* 84, 277–359.
- Chaudhri, O., Small, C., and Bloom, S. (2006). Gastrointestinal hormones regulating appetite. *Philos. Trans. R. Soc. Lond. B Biol. Sci.* 361, 1187–1209.
- Cheng, C.Y., Chu, J.Y., and Chow, B.K. (2011). Central and peripheral administration of secretin inhibits food intake in mice through the activation of the melanocortin system. *Neuropsychopharmacology* 36, 459–471.
- Chondronikola, M., Volpi, E., Børsheim, E., Porter, C., Annamalai, P., Enerbäck, S., Lidell, M.E., Saraf, M.K., Labbe, S.M., Hurren, N.M., et al. (2014). Brown adipose tissue improves whole-body glucose homeostasis and insulin sensitivity in humans. *Diabetes* 63, 4089–4099.
- Chu, J.Y., Cheng, C.Y., Sekar, R., and Chow, B.K. (2013). Vagal afferent mediates the anorectic effect of peripheral secretin. *PLoS ONE* 8, e64859.
- Curtis, P.J., Fender, H.R., Rayford, P.L., and Thompson, J.C. (1976). Disappearance half-time of endogenous and exogenous secretin in dogs. *Gut* 17, 595–599.
- Dicker, A., Zhao, J., Cannon, B., and Nedergaard, J. (1998). Apparent thermogenic effect of injected glucagon is not due to a direct effect on brown fat cells. *Am. J. Physiol.* 275, R1674–R1682.
- Dong, M., Te, J.A., Xu, X., Wang, J., Pinon, D.I., Storzjohann, L., Bordner, A.J., and Miller, L.J. (2011). Lactam constraints provide insights into the receptor-bound conformation of secretin and stabilize a receptor antagonist. *Biochemistry* 50, 8181–8192.
- Fischer, A.W., Cannon, B., and Nedergaard, J. (2018). Optimal housing temperatures for mice to mimic the thermal environment of humans: An experimental study. *Mol. Metab.* 7, 161–170.
- Glick, Z. (1982). Inverse relationship between brown fat thermogenesis and meal size: the thermostatic control of food intake revisited. *Physiol. Behav.* 29, 1137–1140.
- Glick, Z., Teague, R.J., and Bray, G.A. (1981). Brown adipose tissue: thermic response increased by a single low protein, high carbohydrate meal. *Science* 213, 1125–1127.
- Grujic, D., Susulic, V.S., Harper, M.E., Himms-Hagen, J., Cunningham, B.A., Corkey, B.E., and Lowell, B.B. (1997). Beta3-adrenergic receptors on white and brown adipocytes mediate beta3-selective agonist-induced effects on energy expenditure, insulin secretion, and food intake. A study using transgenic and gene knockout mice. *J. Biol. Chem.* 272, 17686–17693.
- Hanssen, M.J., Hoeks, J., Brans, B., van der Lans, A.A., Schaart, G., van den Driessche, J.J., Jörgensen, J.A., Boekschoten, M.V., Hesselink, M.K., Havkes, B., et al. (2015). Short-term cold acclimation improves insulin sensitivity in patients with type 2 diabetes mellitus. *Nat. Med.* 21, 863–865.
- Himms-Hagen, J. (1995). Role of brown adipose tissue thermogenesis in control of thermoregulatory feeding in rats: a new hypothesis that links thermostatic and glucostatic hypotheses for control of food intake. *Proc. Soc. Exp. Biol. Med.* 208, 159–169.
- Jeong, J.H., Lee, D.K., Liu, S.M., Chua, S.C., Jr., Schwartz, G.J., and Jo, Y.H. (2018). Activation of temperature-sensitive TRPV1-like receptors in ARC POMC neurons reduces food intake. *PLoS Biol.* 16, e2004399.
- Klingenspor, M. (2003). Cold-induced recruitment of brown adipose tissue thermogenesis. *Exp. Physiol.* 88, 141–148.
- Kozak, L.P. (2010). Brown fat and the myth of diet-induced thermogenesis. *Cell Metab.* 11, 263–267.
- Li, Y., Fromme, T., and Klingenspor, M. (2017). Meaningful respirometric measurements of UCP1-mediated thermogenesis. *Biochimie* 134, 56–61.
- Li, Y., Fromme, T., Schweizer, S., Schöttl, T., and Klingenspor, M. (2014). Taking control over intracellular fatty acid levels is essential for the analysis of thermogenic function in cultured primary brown and brite/beige adipocytes. *EMBO Rep.* 15, 1069–1076.
- Maurer, S.F., Fromme, T., Grossman, L.I., Hüttemann, M., and Klingenspor, M. (2015). The brown and brite adipocyte marker Cox7a1 is not required for non-shivering thermogenesis in mice. *Sci. Rep.* 5, 17704.
- Mayer, J. (1953). Glucostatic mechanism of regulation of food intake. *N. Engl. J. Med.* 249, 13–16.
- Rampone, A.J., and Reynolds, P.J. (1991). Food intake regulation by diet-induced thermogenesis. *Med. Hypotheses* 34, 7–12.
- Reber, J., Willershäuser, M., Karlas, A., Paul-Yuan, K., Diot, G., Franz, D., Fromme, T., Ovsepien, S.V., Bézière, N., Dubikovskaya, E., et al. (2018). Non-invasive Measurement of Brown Fat Metabolism Based on Optoacoustic Imaging of Hemoglobin Gradients. *Cell Metab.* 27, 689–701.e4.
- Rosen, E.D., and Spiegelman, B.M. (2006). Adipocytes as regulators of energy balance and glucose homeostasis. *Nature* 444, 847–853.
- Rothwell, N.J., and Stock, M.J. (1979). A role for brown adipose tissue in diet-induced thermogenesis. *Nature* 281, 31–35.
- Ryu, V., Garretson, J.T., Liu, Y., Vaughan, C.H., and Bartness, T.J. (2015). Brown adipose tissue has sympathetic-sensory feedback circuits. *J. Neurosci.* 35, 2181–2190.
- Saito, M. (2013). Brown adipose tissue as a regulator of energy expenditure and body fat in humans. *Diabetes Metab. J.* 37, 22–29.
- Sekar, R., and Chow, B.K. (2014a). Secretin receptor-knockout mice are resistant to high-fat diet-induced obesity and exhibit impaired intestinal lipid absorption. *FASEB J.* 28, 3494–3505.
- Sekar, R., and Chow, B.K.C. (2014b). Lipolytic actions of secretin in mouse adipocytes. *J. Lipid Res.* 55, 190–200.
- Sidossis, L., and Kajimura, S. (2015). Brown and beige fat in humans: thermogenic adipocytes that control energy and glucose homeostasis. *J. Clin. Invest.* 125, 478–486.
- Strader, A.D., and Woods, S.C. (2005). Gastrointestinal hormones and food intake. *Gastroenterology* 128, 175–191.

- Susulic, V.S., Frederich, R.C., Lawitts, J., Tozzo, E., Kahn, B.B., Harper, M.E., Himms-Hagen, J., Flier, J.S., and Lowell, B.B. (1995). Targeted disruption of the beta 3-adrenergic receptor gene. *J. Biol. Chem.* *270*, 29483–29492.
- Thörne, A., and Wahren, J. (1989). Beta-adrenergic blockade does not influence the thermogenic response to a mixed meal in man. *Clin. Physiol.* *9*, 321–332.
- U Din, M., Saari, T., Raiko, J., Kudomi, N., Maurer, S.F., Lahesmaa, M., Fromme, T., Amri, E.Z., Klingenspor, M., Solin, O., et al. (2018). Postprandial Oxidative Metabolism of Human Brown Fat Indicates Thermogenesis. *Cell Metab.* *28*, 207–216.e3.
- Valet, P., Berlan, M., Beauville, M., Crampes, F., Montastruc, J.L., and Lafontan, M. (1990). Neuropeptide Y and peptide YY inhibit lipolysis in human and dog fat cells through a pertussis toxin-sensitive G protein. *J. Clin. Invest.* *85*, 291–295.
- van der Lans, A.A., Hoeks, J., Brans, B., Vijgen, G.H., Visser, M.G., Vosselman, M.J., Hansen, J., Jörgensen, J.A., Wu, J., Mottaghy, F.M., et al. (2013). Cold acclimation recruits human brown fat and increases nonshivering thermogenesis. *J. Clin. Invest.* *123*, 3395–3403.
- Virtanen, K.A., Lidell, M.E., Orava, J., Heglind, M., Westergren, R., Niemi, T., Taittonen, M., Laine, J., Savisto, N.J., Enerbäck, S., and Nuutila, P. (2009). Functional brown adipose tissue in healthy adults. *N. Engl. J. Med.* *360*, 1518–1525.
- Vosselman, M.J., Brans, B., van der Lans, A.A., Wierts, R., van Baak, M.A., Mottaghy, F.M., Schrauwen, P., and van Marken Lichtenbelt, W.D. (2013). Brown adipose tissue activity after a high-calorie meal in humans. *Am. J. Clin. Nutr.* *98*, 57–64.
- Welle, S., Lilavivat, U., and Campbell, R.G. (1981). Thermic effect of feeding in man: increased plasma norepinephrine levels following glucose but not protein or fat consumption. *Metabolism* *30*, 953–958.
- West, D.B., Williams, R.H., Braget, D.J., and Woods, S.C. (1982). Bombesin reduces food intake of normal and hypothalamically obese rats and lowers body weight when given chronically. *Peptides* *3*, 61–67.
- Williams, D.L., Baskin, D.G., and Schwartz, M.W. (2009). Evidence that intestinal glucagon-like peptide-1 plays a physiological role in satiety. *Endocrinology* *150*, 1680–1687.
- Yoneshiro, T., Aita, S., Matsushita, M., Kayahara, T., Kameya, T., Kawai, Y., Iwanaga, T., and Saito, M. (2013). Recruited brown adipose tissue as an anti-obesity agent in humans. *J. Clin. Invest.* *123*, 3404–3408.
- Zwillich, C., Martin, B., Hofeldt, F., Charles, A., Subryan, V., and Burman, K. (1981). Lack of effects of beta sympathetic blockade on the metabolic and respiratory responses to carbohydrate feeding. *Metabolism* *30*, 451–456.

STAR★METHODS

KEY RESOURCES TABLE

REAGENT or RESOURCE	SOURCE	IDENTIFIER
Antibodies		
anti-Secretin	Phoenix Pharmaceuticals	Cat# G-067-04; RRID: AB_2650428
anti-UCP1	Custom made	N/A
anti-GFP	ThermoFischer	Cat# A-11122; RRID: AB_221569
anti-ACTIN	Millipore	Cat# MAB1501; RRID: AB_2223041
anti-SCTR	Sigma-Aldrich	Cat# HPA007269-100UL; RRID: AB_1856640
Bacterial and Virus Strains		
NEB5 α competent <i>E. coli</i>	NEB	Cat# C2988J
Chemicals, Peptides, and Recombinant Proteins		
Arterenol	Sanofi	1mg/ml
Isobutylmethylxanthine	Sigma-Aldrich	Cat# I5879
Indomethacin	Sigma-Aldrich	Cat# I7378
Dexamethasone	Sigma-Aldrich	Cat# D4902
Insulin	Sigma-Aldrich	Cat# I9278-5ML
T3	Sigma-Aldrich	Cat# T6397
Propranolol hydrochlorid	Sigma-Aldrich	Cat# P8688
Bovine serum albumin (BSA) Fatty Acid Free	Sigma-Aldrich	Cat# A3803-100G
Isoproterenol	Sigma-Aldrich	Cat# I6504-100MG
Oligomycin	Sigma-Aldrich	Cat# O4876-5mg
Antimycin A	Sigma-Aldrich	Cat# A8674
Collagenase A	Biochrom	Cat# C 1-22
FCCP	Sigma-Aldrich	Cat# C2920-10MG
Secretin	Tocris	Cat# No.1919
H89 dihydrochloride	Tocris	Cat# No.2910
Atglistatin	Gift from Robert Zimmermann (University of Graz)	N/A
Hi 76-0079	Gift from Robert Zimmermann (University of Graz)	N/A
SensiMix SYBR no Rox	BioLine	Cat# QT650-20
DMEM	Sigma-Aldrich	Cat# D5796
Fetal bovine serum (FBS)	Biochrom	Cat# S0615
TRISure	Bioline	Cat# BIO-38033
Human secretin	This study	N/A
Modified human secretin analog	This study	N/A
GLP1 analog (CEX51)	This study	N/A
Critical Commercial Assays		
SV Total RNA Isolation System	Promega	Cat# Z3105
Pierce BCA Protein Assay Kit	Pierce	Cat# PI-23225
SensiFast cDNA Synthesis Kit	BioLine	Cat# BIO-65054
SensiMix Sybr no Rox	BioLine	Cat# QT650-20
Secretin ELISA kit	Cloud-clone	Cat# CEB075Mu, CEB075Hu
Dual luciferase reporter assay	Promega	Cat# E1960
Seahorse XF96 fluxPak	Seahorse Bioscience	Cat# 102310-001
TruSeq Stranded Total RNA Library Prep Kit	Illumina	Cat# RS-122-2102

(Continued on next page)

Continued

REAGENT or RESOURCE	SOURCE	IDENTIFIER
Deposited Data		
Brown fat RNA-seq data	This paper	GEO: GSE119452, GSM3374837, GSM3374838, GSM3374839, GSM3374840
Experimental Models: Cell Lines		
HEK293	DSMZ	Cat# ACC 305
Primary murine brown and white cells	This paper	N/A
Experimental Models: Organisms/Strains		
Mouse: C57BL/6J	Jackson Laboratory	JAX Stock No:000664
Mouse: 129S-Ucp1 ^{tm1Kz} /J	Jackson Laboratory	JAX Stock No:017476
Mouse: 129S6/SvEVTac	Taconic Biosciences	129SVE
Mouse: Athymic Nude-Foxn1 ^{nu}	Envigo	Athymic Nude-Foxn1 ^{nu}
Oligonucleotides		
siRNA targeting sequence: Sctr #1: CCUGCUGAUCCUCUCUUU	This paper	N/A
siRNA targeting sequence: Sctr #2: CCCUGUCCAACUUAUCAAA	This paper	N/A
siRNA targeting sequence: Sctr #3: CCAUCGUGAUCAAUUUCAU	This paper	N/A
Primers for qPCR, see detailed methods	This paper	N/A
Recombinant DNA		
pCMV-murine SCTR expressing vector	This paper	N/A
pAD-CRE luciferase reporter vector	This paper	N/A
phRG-B-Renilla luciferase vector	Promega	Cat# E6281
Software and Algorithms		
GraphPad Prism 6	Graphpad Software	N/A
Genomatix Software Suite	Genomatix AG	N/A
MATLAB	Mathworks	N/A
Other		
TSE LabMaster	TSE Systems	N/A
FoxBox	Sable Systems	N/A
G2 E-Mitter	Starr Life Sciences	N/A
MSOT imaging system inVision 256-TF	iThera Medical GmbH	N/A
XF96 Extracellular Flux Analyzer	Seahorse Bioscience	N/A
ER4000 Energizer/Receiver	Starr Life Sciences	N/A
Lightcycler II	Roche	N/A

CONTACT FOR REAGENT AND RESOURCE SHARING

Further information and requests for resources and reagents should be directed to and will be fulfilled by the Lead Contact, Martin Klingenspor (mk@tum.de).

EXPERIMENTAL MODEL AND SUBJECT DETAILS**Animals**

Animal experiments were approved by the German animal welfare authorities at the district government (approval no. 55.2-1-54-2532-34-2016 and 55.2-1-54-2532-123-2013). Mice were bred at the specific-pathogen free animal facility of Technical University of Munich. They had *ad libitum* access to food and water and were maintained at 22 ± 1°C and 50%–60% relative humidity in a 12 h:12 h light:dark cycle. Male 129S6/SvEv mice, aged 5 to 6 wk were used for primary cultures of brown and white adipocytes. Male C57BL/6J, male C57BL6/N mice, male 129S1/SvImJ mice (UCP1-KO mice and wild-type littermates) and male 129S6/SvEV

were used for the *in vivo* experiments. Athymic female Nude-Foxn1^{nu} mice, aged 13 wk at the beginning of the experiments were obtained from Envigo and kept at 24 ± 1°C with *ad libitum* access to food and water at the Helmholtz Zentrum München.

Primary cell culture

Adipose tissues were dissected from 5 week-old 129S6/SvEV mice or 129S1/SvImJ mice (UCP1-KO mice and wild-type littermates) ($n = 2$ per experiment, pooled) and digested with collagenase as described previously (Li et al., 2014). Floating mature adipocytes were harvested for gene expression analysis. Stromal vascular fraction (SVF) cells were either harvested or plated in 12-well plates, and adherent cells were grown to confluence. Cells were differentiated into adipocytes as previously described. Briefly, cells were cultured for 2 days with 5 µg/ml insulin, 1 nM 3,3',5-triiodo-L-thyronine (T3), 125 µM indomethacin, 0.5 mM isobutylmethylxanthine (IBMX) and 1 µM dexamethasone in adipocyte culture media (DMEM supplemented with 10% heat-inactivated FBS, penicillin/streptomycin). Cells were then maintained in adipocyte culture media supplemented with 5 µg/ml insulin and 1 nM T3 for 6 days, with fresh media replacement every 2 days. Cells were harvested on day 7 with or without 6h secretin (500nM) treatment in TRISure.

Human study

Human experiments were performed in Turku PET Centre in Finland as part of two separate PET/CT imaging study cohorts. The ethical committee of South-Western Finland Hospital District evaluated and approved the studies, and all participants gave their written informed consent before any study procedures (Clinical trial number: NCT03290846).

Serum secretin levels were measured in seventeen healthy volunteers (13 females and 4 males; 36.3 ± 9.5 years; BMI 27.2 ± 2.9), who participated in a study where post-prandial BAT oxygen consumption and fatty acid uptake were measured using 15O-O2 and 18F-FTHA PET/CT, respectively. Blood samples for secretin measurement were drawn at baseline (overnight fasting) and 30-40 minutes after completing a mixed meal consisting of 542 kcal (58% carbohydrates, 25% fat, 17% protein). Concurrent dynamic PET imaging of supraclavicular and upper thoracic region was performed during postprandial state.

Effects of secretin on BAT glucose metabolism was evaluated in a separate group of lean, healthy males ($n = 7$, mean age 46.6 ± 11.9 years; mean BMI 23.7 ± 2.0). Studies were done twice, after two short intravenous infusions of secretin hydrochloride (Secrelux, 1IU/kg each) or saline (placebo) using single-blinded randomization. Dynamic PET-CT scans of the neck area, were done using 18F-FDG and analyzed as described earlier (Virtanen et al., 2009).

METHOD DETAILS

RNA-sequencing

Total RNA isolated from BAT samples of male C57BL/6J mice ($n = 4$) housed under room temperature (23°C) was applied to transcriptome analysis by next generation sequencing (RNA-Seq) using Illumina HiSeq 2500 platform (Illumina). Sequencing libraries were prepared using the TruSeq RNA Sample Prep kit v2 (Illumina). Libraries from 4 samples were pooled into one sequencing lane and sequenced using a 50-cycle TruSeq SBS Kit v3-HS (Illumina), resulting in a depth of > 25 million reads/sample. Sequenced tags were aligned to the Ensembl 75 transcriptome annotation (NCBI38/mm10 mouse genome) using Genomatix Software Suite. All genes and transcripts were assigned relative coverage rates as measured in RPKM units ('reads per kilobase per million mapped reads').

Western Blot

For western blot analysis, cells were lysed in RIPA buffer. 30µg of total-cell lysates were separated on 12.5% SDS-PAGE gels, transferred to PVDF membrane (Millipore) by using a Trans-Blot SD. Semi-Dry Transfer Cell (Bio-Rad), and probed with anti-UCP1 (1:10,000), anti-ACTIN (Millipore, 1:10,000) and anti-SCTR (Sigma, 1:300). Secondary antibodies conjugated to IRDye 680 or IRDye 800 (Li-Cor Biosciences) were incubated at a dilution of 1:20,000. Fluorescent images were captured by an Odyssey fluorescent imager (Li-Cor Biosciences).

Gene expression analysis (qRT-PCR)

RNA was extracted from cultured cells or frozen tissue samples (129S6/SvEV) using TRIsure, purified with SV Total RNA Isolation System, Promega and reverse transcribed using SensiFAST cDNA Synthesis Kit (BIOLINE). The resultant cDNA was analyzed by qRT-PCR. Briefly, 1 µL of 1:10 diluted cDNA and 400 nmol of each primer were mixed with SensiMix SYBR Master Mix No-ROX (Bioline). Reactions were performed in 384-well format using a lightcycler II instrument (Roche). Standard reactions containing serial diluted pooled cDNA of all samples (Pure, 1:2, 1:4, 1:8, 1:16, 1:32 and 1:64) as a template were used to establish a standard curve, from which gene expression levels of samples were calculated. The RNA abundance of each gene was normalized to a housekeeping gene *Gtf2b*. The following primers were used:

Ucp1 F: 5'-GTACACCAAGGAAGGACCGA-3', R: 5'-TTTATTCGTGGTCTCCCAGC-3';
 Sctr F: 5'-ATGCACCTGTTTGTGCCTT-3', R: 5'-TAGTTGGCCATGATGCAGTA-3';
 Gtf2b F: 5'-TGGAGATTTGCCACCATGA-3', R: 5'-GAATTGCCAAACTCATCAAAACT-3';
 Pref1 F: 5'-AGTACGAATGCTCCTGCACAC-3', R: 5'-CTGGCCCTCATCATCCAC-3';
 Fgf21 F: 5'-AGATCAGGGAGGATGGAACA-3', R: 5'-TCAAAGTGAGGCGATCCATA-3';

Fabp4 F: 5'-GATGGTGACAAGCTGGTGGT-3', R: 5'-TTTATTTAATCAACATAACCATATCCA-3';
 PGC1a F: 5'-GGACGGAAGCAATTTTCAA-3', R: 5'-GAGTCTTGGGAAAGGACACG-3';
 Dio2 F: 5'-TGTCTGGAACAGCTTCCTCC-3', R: 5'-AGTGAAAGGTGGTCAGGTGG-3';
 Pparg F: 5'-TCAGCTCTGTGGACCTCTCC -3', R: 5'-ACCCCTTGCATCCTTACAAG-3';
 Agrp F: 5'-GTCTAAGTCTGAATGGCCTCAAG-3', R: 5'-CATCCATTGGCTAGGTGCGAC-3';
 Pomc F: 5'-CCCTCCTGCTCAGACCTC-3', R: 5'-CGTTGCCAGGAAACACGG-3';
 Npy F: 5'-CTGACCCTCGCTCTATCTCTGC-3' R: 5'-CCATCACCACATGGAAGGGTCT-3'
 Cart F: 5'-CGAGCCCTGGACATCTACTCTG-3' R: 5'-TCTTTGCACACACCAACACC-3'
 Bdnf F: 5'-TGGTATGACTGTGCATCCCAGG-3' R: 5'-TCACCCGGGAAGTGTACAAGTC-3'
 Pacap F: 5'-ACCAATGACCATGTGTAGCGGA-3' R: 5'-CCATTTGTTTTCGGTAGCGGCT-3'
 Trpv-1 F: 5'-ATCTTACCACGGCTGCTTACT-3' R: 5'-TCCTTGCGATGGCTGAAGTACA-3'

Respiration assays

The cellular oxygen consumption rate (OCR) of primary adipocytes was determined using an XF96 Extracellular Flux Analyzer (Seahorse Bioscience) as described previously (Li et al., 2014). Briefly, primary adipocytes were cultured and differentiated in XF96 microplates. At day 7 of differentiation, cells were washed once with prewarmed, unbuffered assay medium (DMEM basal medium supplemented with 25 mM glucose, 31 mM NaCl, 2 mM GlutaMax and 15 mg/l phenol red, pH 7.4) (basal assay medium) and then the medium was replaced with basal assay medium containing 1%–2% essentially fatty acid free bovine serum albumin (BSA), and incubated at 37°C in a room air incubator for 1 h. The drug injection ports of the sensor cartridges were loaded with the assay reagents at 10X in basal assay medium (no BSA). Basal respiration was measured in untreated cells. Coupled respiration was inhibited by oligomycin treatment (5 μM). UCP1 mediated uncoupled respiration was determined after isoproterenol or secretin stimulation. Maximum respiratory capacity was assessed after FCCP (Sigma-Aldrich) addition (1 μM). Finally, mitochondrial respiration was blocked by antimycin A (Sigma-Aldrich) (5 μM) treatment and the residual OCR was considered non-mitochondrial respiration. For some experiments, cells were pretreated with 50 μM H89 (PKA inhibitor), 1 – 100 μM propranolol (β-adrenergic receptor antagonist), 40 μM Atglistatin (ATGL inhibitor) and 40 μM Hi76-0079 (HSL inhibitor), or reverse transfected with small interfering RNAs (siRNAs) targeting SctR (#1CCUGCUGAUCCCUCUCUUU; #2CCCUGUCCAACUUAUCAA; #3CCAUCGUGAU CAUUUUAU) and nontargeting control siRNA (UUUGUAAUCGUC GAUACCC) as described previously (Li et al., 2017) before bioenergetic profiling. Oxygen consumption rates were automatically calculated by the Seahorse XF-96 software. Each experiment was repeated at least 3 times with similar results.

Surgical implantation of telemetry transmitters

To monitor interscapular BAT temperature, telemetry transmitters (G2 E-Mitter, Starr Life Sciences Corp., Oakmont, PA, USA) were implanted above the interscapular BAT in 10-weeks-old 129S6/SvEv mice (n = 24). Mice were anesthetized by combined i.p. injection of medetomidine (0.5 mg/kg), midazolam (5 mg/kg) and fentanyl (0.05 mg/kg). The interscapular region was opened by a small incision and the transmitter was placed above the interscapular BAT pad. The incision was closed with surgical adhesive. Atipamezole (2.5 mg/kg), flumazenil (0.5 mg/kg) and naloxone (1.2 mg/kg) were injected subcutaneously to terminate anesthesia. In addition, mice received 10 mg/kg rimadyl and were singly housed in the post-operative recovery period for 4–5 days.

Monitoring of food intake and iBAT temperature

Food intake (FI) was recorded in individually housed mice using an automated monitoring system (TSE LabMaster Home Cage Activity, Bad Homburg, Germany). The food baskets were connected to high precision balances to record FI. A receiver plate (ER4000 Energizer/Receiver, Oakmont, PA, USA) underneath the cage recorded interscapular BAT temperature (T_{iBAT}) signals of the implanted transmitter. Food basket weight and T_{iBAT} were averaged in 5 min intervals. Mice were habituated to the cages with daily i.p. PBS injections for three days ahead of the experiment start, after which food was removed from the cages at 5pm and mice were fasted for overnight. In the next morning, mice were i.p. injected either PBS or secretin (5 nmol/mouse) and food intake was monitored during the following 72hs. For endogenous secretin blocking experiment, mice were s.c. injected with either anti-GFP or anti-secretin antibody at the time when food was removed. Postprandial secretin serum levels (Figure 3a) as well as *in vitro* testing results for blocking efficiency of the anti-secretin antibody (Phoenix Pharmaceuticals, G-067-04) (Figure S5) were used to estimate the appropriate concentration of antibody to block endogenous secretin activity during refeeding. Assuming a total blood volume of 2 ml/mouse, 400 pmol anti-secretin antibody were injected per mouse. Propranolol (10mg/kg BW) or PBS was i.p. injected 20 min prior to secretin or PBS in the β-blockage experiment.

Indirect calorimetry

Indirect calorimetry was based on an open respirometer system (LabMaster System; TSE Systems, Bad Homburg, Germany) and was performed as described previously (Maurer et al., 2015). Mice were placed in metabolic cages (3L volume) without food and water, transferred to a climate cabinet (TPK 600, Feutron, Greiz/Germany) preconditioned to 30 °C and connected to the indirect calorimetry setup (Phenomaster, TSE Systems, Bad Homburg/Germany) to measure basal metabolic rate (BMR) during fasting (8:00 am–12:00 pm). The air from the cages was extracted over a period of 1 min every 7 min with a flow rate of 33 l/h, dried in a

cooling trap and analyzed for O₂ content. O₂ consumption [ml/h] was calculated via comparison of the air from the cages with the air from an empty reference cage. BMR [ml O₂/h] was calculated as the lowest mean of three consecutive oxygen consumption values. After BMR measurements, mice were i.p. injected either PBS or secretin (0.5mg/kg) and measured in the calorimetry chamber for about one hour with a high-resolution recording of 10 s intervals at 27 °C to avoid secretin induced hyperthermia. Metabolic rates were converted into heat production (HP [mW] = (4.44+1.43*respiratory exchange ratio)*oxygen consumption [ml/h]).

Macroscopic multi-spectral optoacoustic tomography (MSOT) combined with indirect calorimetry

Real-time multi-spectral optoacoustic tomography (MSOT) mouse measurements were conducted with an MSOT small animal imaging system (inVision 256-TF, iThera Medical GmbH, Munich, Germany) as described previously (Reber et al., 2018). Athymic female Nude-Foxn1^{nu} mice were anesthetized by i.p. injection of 75 mg/kg pentobarbital (Narcoren, Merial GmbH, Germany) and placed in the MSOT system. To induce and image BAT activation, secretin (5 nmol) was administered via a catheter inserted in the mouse tail vein. Before, during, and after the activation period images were acquired at 25 different wavelengths: from 700 nm to 900 nm, with a step increment of 10 nm providing multi-spectral anatomic and functional information in a real-time and label-free mode. In parallel O₂ and CO₂ were analyzed in 1 s intervals using a transportable indirect calorimetry system (FoxBox, Sable Systems International, USA) and later converted into HP. For this compressed air from a bottle was pulled through the MSOT mouse holder with a flow rate of 700ml/min using the pump of the FoxBox. After the mouse holder air was dried by a cooling trap and magnesium perchlorate (Merck KGaA, Germany) and passing a filter (Model 9922-11, Parker Balston) before entering gas analysis. Gas composition of the empty mouse holder was analyzed before and after measuring the mouse and used for drift correction. Drift correction and data analysis was performed with the software ExpeData (ExpeData version 1.1.22, Sable Systems International, USA). HP before reflects the mean of the 5 min interval before injection and HP after the mean maximum HP in a 1 min interval measured after injection. The data analysis for MSOT measurements consisted of the calculation of the total blood volume (TBV = oxygenated hemoglobin (HbO₂) + deoxygenated hemoglobin (Hb)) and the oxygen saturation (SO₂ = HbO₂/TBV).

Analysis of food intake data

Food intake was calculated as first derivative of cumulative food intake obtained from automated monitoring system (TSE LabMaster Home Cage Activity, Bad Homburg, Germany). Food intake greater than 0.005 g and separated by intermeal bout length greater or equal 15 min where defined as meal. Mean meal duration and mean intermeal bout length were calculated as mean of individual means.

Measurement of plasma secretin concentrations

Blood was collected at the time the mouse was killed. Plasma secretin levels were determined by ELISA using the kit purchased from Cloud-Clone following the manufacturer's instructions. Concentrations were calculated using a standard curve generated by secretin standards included in the kit.

Hypothalamic neuropeptides gene expression analysis

Male 129S1/SvImJ mice (UCP1 WT and KO) were fasted overnight and i.p. injected either PBS or secretin (5 nmol/mouse). After 4h of treatment, hypothalamic tissues were dissected, snap-frozen and later subjected to RNA extraction and gene expression analysis. In a second experiment, male 129S6/SvEV mice were fasted overnight and subsequently put into a climate chamber where they were exposed to room temperature or to moderate heat. In case of the heat exposure, environmental temperature has been raised from 34°C to 37°C with one degree per hour resulting in a total exposure time of 4 hours. Afterward hypothalamic tissue and preoptical region were separately dissected followed by the same procedure as in the previous experiment.

Diet-induced obese mice study

All diet-induced obese (DIO) mice studies have been approved by Eli Lilly and Company's Institutional Animal Care and Use Committee.

Human secretin (1-27 amide: HSDGTFTSELSRLREGARLQRLQGLV-amide; native secretin) and modified human secretin analog (1-27 amide: HSDGTFTSELSRLREE*ARLK*RLLQGLV-amide; modified secretin) (Dong et al., 2011) that contains a lactam bridge between side chains of Glu16 and Lys20 were synthesized by solid-phase peptide synthesis using established chemical protocols. After cleavage from the solid support and purification using reversed-phase chromatography, the lyophilized powders as trifluoroacetate salts were formulated in aqueous buffer.

Diet-induced obese (DIO) male C57BL6/N mice (Taconic Biosciences, Cambridge City, IN) 30 to 31 weeks old, maintained on a calorie rich diet since arrival at Lilly (TD95217; Teklad, Madison, WI), were used in the study. Mice were individually housed in a temperature-controlled (24°C) facility with 12 hour light/dark cycle (lights on 2200) and free access to food (TD95217) and water. After a minimum of 2 weeks acclimation to the facility, the mice were randomized according to their body weight, so each experimental group of animals would have similar body weight. The body weights ranged from 46 to 54 g. Vehicle (20 mM Citrate at pH 5.5), native secretin (166 nmol/kg/day) or modified secretin (163 nmol/kg/day) dissolved in vehicle was administered by subcutaneous (SC) mini-osmotic pump (Alzet, Model 2002; Durect Corporation, Cupertino, CA) as a SC infusion (12 µl/mouse/day) to *ad libitum* fed DIO mice throughout the study period. Body weight and food intake were monitored daily. Absolute changes in body weight were

calculated by subtracting the body weight of the same animal on the first day of the treatment. On Days 1 and 14, total fat mass and total water mass were measured by quantitative nuclear magnetic resonance (QNM) using an Echo Medical System (Houston, TX) instrument. Fat-free mass was calculated as body weight – fat mass. For the thermoneutral experiment, mice were acclimatized to 30°C one week before the experiment started. All other study conditions were kept, except the dosage. Native secretin was administered in a concentration of 996 nmol/kg/day and modified secretin of 326 nmol/kg/day. In addition to body weight and food intake, oxygen consumption was also measured.

Dual luciferase reporter assay

Blocking potential of the anti-secretin-antibody was determined by measuring secretin receptor activation in response to variable ratios of secretin and anti-secretin antibody. Secretin receptor activity was quantified using a dual luciferase reporter system based on cAMP response element (CRE) driven firefly luciferase (CRE-PLuc; *Photinus pyralis*) and constitutive Renilla luciferase (RLuc; *Renilla reniformis*). HEK293 cells were transiently transfected with CRE-PLuc, RLuc, and Sctr. Secretin receptor activity was quantified as the ratio of bioluminescence of firefly (PLuc) and renilla (RLuc) luciferase.

QUANTIFICATION AND STATISTICAL ANALYSIS

Two-tailed Student's *t* tests were used for single comparisons and analysis of variance (ANOVA) with Tukey's post hoc tests for multiple comparisons. PET/CT analysis was analyzed using paired one-tailed *t* test. *P* values below 0.05 were considered significant. Statistical analysis was performed with GraphPad prism 6 software. All data are represented as mean ± SD.

All linear mixed effect models were calculated with the *fitlme* function of MATLAB R2016b (Mathworks). Specifically, cumulative food intake was analyzed by means of linear mixed effect models with the fixed effects 'time' and 'treatment group', their interaction, and 'individual' as random effect. Additionally, we applied a more sophisticated model to specifically detect an effect of secretin on metabolic rate from cumulative food intake data by including the additional random factors 'initial body mass' (to capture the metabolic requirements of the mouse) and 'overall change in body mass' (to capture the alternate fate of food, i.e., fat deposition/loss).

DATA AND SOFTWARE AVAILABILITY

The accession number for the RNA-Seq data presented in this article is GEO: GSE119452.



Figure S1. BioGPS Data for *Sctr* Expression in 96 Mouse Tissues and Purified Mouse Cell Population, Related to Figure 1
Sctr (secretin receptor) expression data were retrieved from the BioGPS database (<http://biogps.org/#goto=genereport&id=319229>) and expressed as fold over the median (M). *Sctr* is most abundant in neuroblastoma cell line (Neuro2a), followed by brown adipose tissue, placenta and stomach.

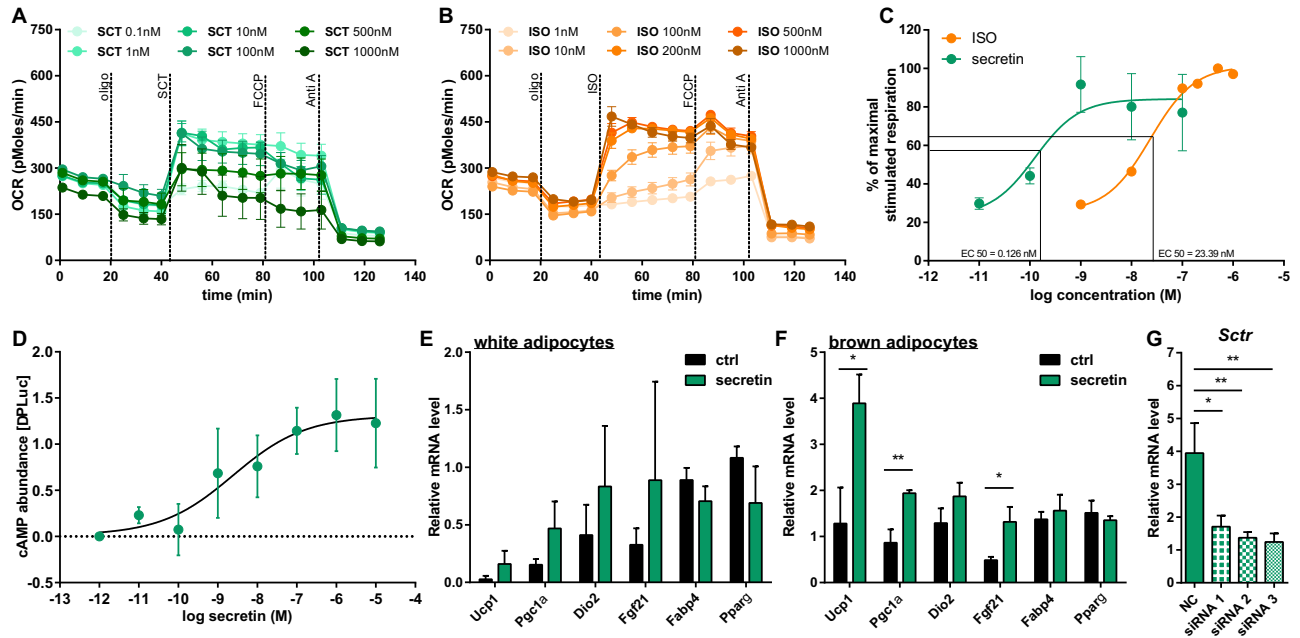


Figure S2. Effects of Secretin on Both Thermogenic Activity and Capacity in Primary Brown and White Adipocytes, Related to Figure 2

(A–C) Microplate-based respirometry of primary brown adipocytes according to the following protocol. After assessment of basal oxygen consumption oligo (oligomycin) was injected to determine basal leak respiration. Next, different doses of either ISO (isoproterenol, 1nM–1 μ M) or SCT (secretin, 0.1nM–1 μ M) were added to stimulate UCP1-mediated uncoupled respiration. By adding of FCCP maximal leak respiration was determined. Lastly, non-mitochondrial oxygen consumption was assessed by injecting Anti A (antimycin A). Representative time-course of oxygen consumption rates (OCR) of primary brown adipocytes stimulated with different doses of either (A) secretin ($n = 3$) or (B) ISO ($n = 1$). (C) EC_{50} values of secretin and ISO in stimulating the maximal UCP1-mediated uncoupled respiration. The maximal stimulated respiration was calculated as fold change over basal leak and was set to 100%. (D) Cytosolic cAMP abundance after stimulation with increasing secretin concentrations for 30 min ($n = 3$) in primary brown adipocytes. (E–F) Effect of secretin (6h) on the expression of thermogenic genes in primary adipocytes derived from interscapular brown (E) and inguinal white (F) adipose tissue determined by qRT-PCR ($n = 3$). *Pgc1 α* : Peroxisome proliferator-activated receptor γ coactivator 1 α ; *Dio-2*: Deiodinase, Iodothyronine Type II; *Fgf21*: Fibroblast growth factor 21; *Fabp4*: Fatty acid binding protein 4; *Ppar γ* : Peroxisome proliferator-activated receptor γ . (G) Relative mRNA expression of *Sctr* (secretin receptor) normalized to *Gtf2b* (General transcription factor IIb) in primary brown adipocytes reverse transfected with either small interfering RNAs (siRNA) targeting *Sctr* or nontargeting controls (NC), respectively. Reverse transfection was performed at day 5 of differentiation ($n = 3$). Analysis was performed at day 8 of differentiation. Data are presented as mean \pm SD (E–F+G) Statistical analysis was conducted using unpaired t test. * $p < 0.05$; ** $p < 0.01$, compared with the control group.

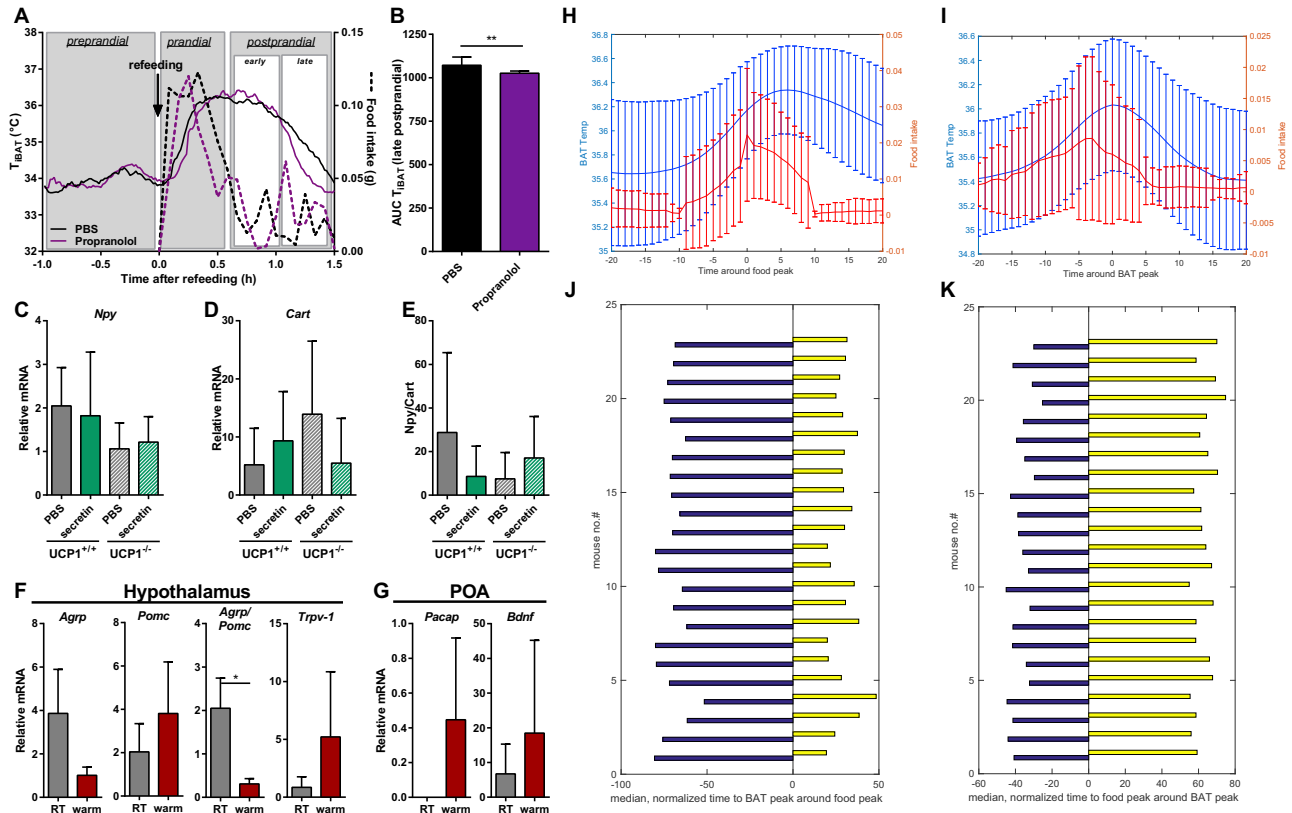


Figure S3. The Close Relationship between Food Intake and Thermogenesis as Evidenced by Hypothalamic Gene Expression and Food Intake Events Analyses, Related to Figure 3

(A-B) Three main different phases of single meal-associated thermogenesis: preprandial, prandial and postprandial (early and late) thermogenesis. Propranolol only decreased the late postprandial thermogenesis. (A) Mean iBAT temperature in response to refeeding after propranolol or PBS pre-treatment (20mins before refeeding). (B) The late postprandial thermogenesis was reduced in response to propranolol pre-treatment, as quantified as area under the curve (AUC) of iBAT temperature. (C-G) Anorexigenic and orexigenic hypothalamic gene expression was regulated by both secretin treatment and short exposure to ambient temperature above thermoneutrality. Relative mRNA level of *Npy* (neuropeptide y) (C) and *Cart* (cocaine and amphetamine regulated transcript) (D) in hypothalamus of fasted UCP1^{+/+} and UCP1^{-/-} mice in response to a single i.p. injection of PBS or secretin (4h) normalized to transcription factor *Gtf2b*. (E) Ratio of *Npy* and *Cart* expression. (F+G) Fasted mice (18h) were placed into a climate chamber and temperature was gradually increased from 34 to 37°C over 4 h and gene expression was analyzed in hypothalamus (F) and preoptic region (G). *AgRP* (agouti-related peptide), *Pomc* (pro-opiomelanocortin), *Trpv-1* (transient receptor potential cation channel subfamily V member 1), *Pacp* (pituitary adenylate cyclase-activating peptide), *Bdnf* (brain-derived neurotrophic factor). Ratio of *AgRP/Pomc*.

(H-K) Relationship between feeding behavior and brown fat thermogenesis during *ad libitum* feeding. In total, we detected 1919 feeding events and 1706 bouts of BAT activity during 70h of continuously monitoring food intake by automatic manger scales and recording iBAT temperature by implanted telemetry sensors on 23 mice in a 1-minute bins resolution. Feeding event and iBAT activity bout were defined based on a peak in the mean of ten consecutive minutes. (H) Mean food intake (red) and iBAT temperature (blue) during 20 minutes preceding and 20 minutes following a feeding event. The initiation of feeding is always accompanied by a rise in iBAT temperature. iBAT temperature reached its maximum approx. 5 minutes after the food intake peak. (I) Mean food intake (red) and iBAT temperature (blue) during 20 minutes preceding and 20 minutes following a BAT activity bout. Peaks in iBAT temperature are associated with a preceding feeding event peaking approx. 5 minutes earlier. (J) In every single mouse of 23 in total, during feeding events, the time span for iBAT temperature to reach a peak after the food peak (yellow bars) was generally shorter compared to the time span before the food peak (blue bars). Bars represent median time spans normalized to individual peak frequency (arbitrary units). This data indicated that a rise in iBAT temperature was plausibly the consequence of food intake. (K) In every single mouse, during BAT activity bouts, the time span preceding the BAT temperature peak to a food intake peak (blue bars) was generally shorter than time span after the BAT temperature peak to the next food peak (yellow bars). Bars represent median time spans normalized to individual peak frequency (arbitrary units). This data indicated that a rise in iBAT temperature could have caused the termination of feeding.

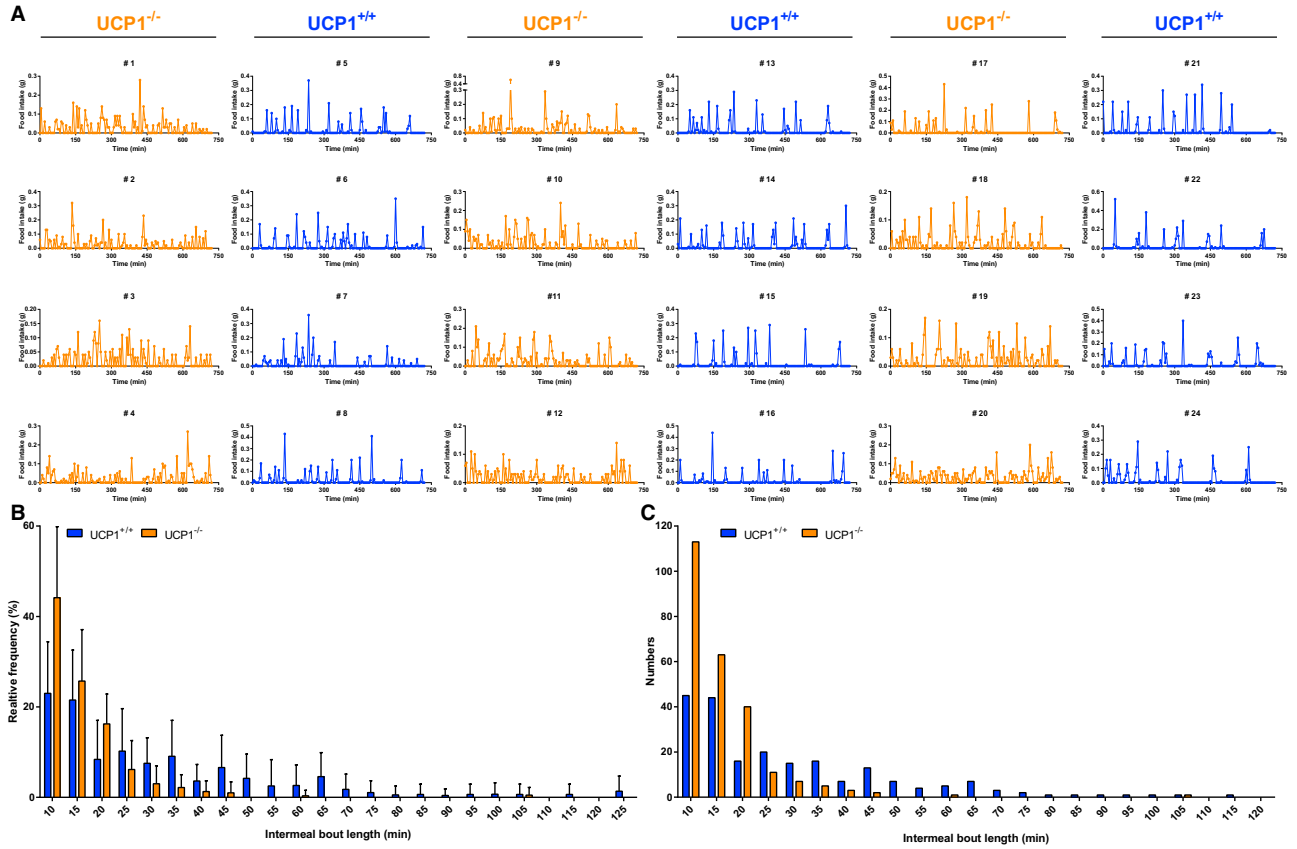


Figure S4. Altered Feeding Patterns in UCP1-KO Mice, Related to Figure 3

Food intake (FI) was recorded in 12 individually housed UCP1^{+/+} (blue) and 12 UCP1^{-/-} (orange) mice (129S1/SvImJ) using an automated monitoring system (TSE LabMaster Home Cage Activity, Bad Homburg, Germany) during one dark phase after acclimatization period of three days. The food baskets were connected to high precision balances to record FI in 5-min bins. (A) Individual feeding over 12 hours during dark phase. (B) Relative distribution frequency of intermeal bout length of UCP1^{+/+} (blue) and UCP1^{-/-} (orange) mice during one dark phase. (C) Numbers of variant intermeal bout length during one dark phase of UCP1^{+/+} (blue) and UCP1^{-/-} (orange) mice. Data are presented as mean ± SD (n = 12).

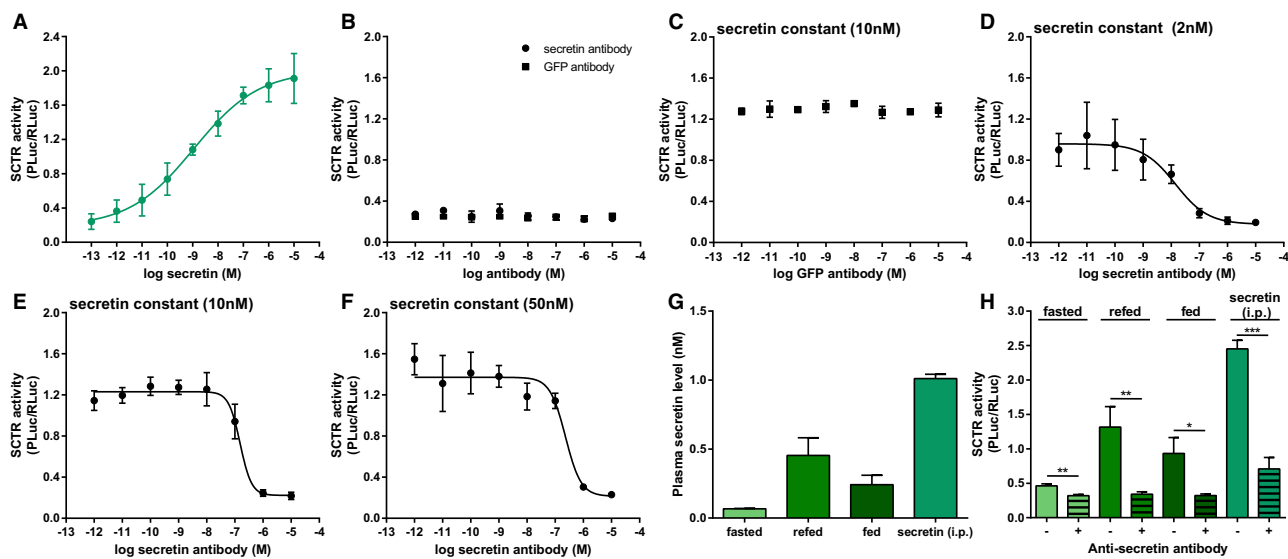


Figure S5. Anti-secretin Antibody Is Capable of Completely Inhibiting Secretin Activity *In Vitro*, Related to Figure 4

The blocking efficiency of anti-secretin antibody on secretin activity was characterized using HEK293 cells expressing triple vectors (SCTR, CRE-PLuc and RLuc). (A) Secretin increased SCTR activity in a dose-dependent manner as reflected by cAMP response element (CRE)-mediated luciferase activity. (B) Increasing concentrations of secretin- or GFP- (green-fluorescent protein) antibody had no effect on SCTR activity. (C) Increasing concentrations of GFP-antibody had no impact on secretin (10nM)-induced SCTR activity. (D–F) Increasing concentrations of secretin-antibody were capable to inhibit secretin-stimulated SCTR activity. A concentration ratio of 100 (antibody/secretin) was able to neutralize secretin activity in stimulating SCTR-cAMP pathway. (G) Secretin concentration was quantified in plasma from mice either fasted, 1h refed after fasting, fed *ad libitum* or 30 min after intraperitoneal injection of 5 nmol secretin based on their capacities in stimulating SCTR activity according to the standard curve in panel A. (H) 30 min incubation with secretin-antibody (630nM) was sufficient to completely inhibit plasma secretin activity. Data was analyzed by paired t test. Data are presented as mean \pm SD (n = 3). ** = $p < 0.01$, *** = $p < 0.001$.

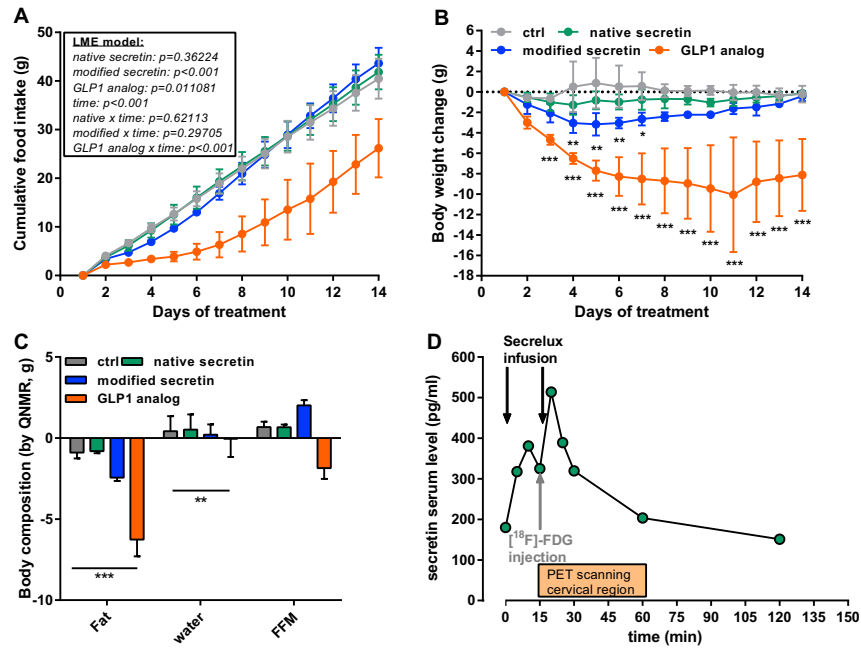


Figure S6. Chronic Infusion of Modified Secretin Transiently Slightly Decreases Food Intake and Body Weight in Diet-Induced Obese Mice at Room Temperature, Related to Figures 5 and 6

(A–C) Vehicle (20mM Citrate), native secretin (166 nmol/kg/day), modified secretin (163 nmol/kg/day) or GLP1 analog (CEX51, 30 nmol/kg/day) dissolved in vehicle was administered by subcutaneous (s.c.) miniosmotic pumps as a s.c. infusion ($12\mu\text{l}/\text{mouse}/\text{day}$) to *ad libitum* fed diet-induced obese (DIO) male C57BL/6N mice throughout the study period ($n=6$). Mice were kept at room temperature. (A) Food intake and (B) body weight were monitored daily. Absolute changes in body weight were calculated by subtracting the body weight of the same animal on the first day of treatment. (C) On day 1 and 14, total fat mass and total water mass were measured by quantitative nuclear magnetic resonance (QNMR). Fat-free mass was calculated as body weight minus fat mass. (D) Two-bolus Secretelux infusion increases serum secretin level in humans. Representative time course of serum secretin level after two-bolus Secretelux infusion (0 min and 15 min). The second Secretelux bolus was administered right after ^{18}F -FDG injection. Subsequently, PET scanning of the cervical region was initiated and glucose uptake was measured for approximately 40 min. (A) was analyzed by linear mixed effects model with fixed effects “treatment,” “time” and interaction between both and with random factor “individual.” (B) was analyzed by two-way ANOVA RM (Tukey’s test). (C) was analyzed by one-way ANOVA (Tukey’s test). * = $p < 0.05$; ** = $p < 0.01$, *** = $p < 0.001$.